International Journal of Vaccine Theory, Practice, and Research

IJVTPR

Real-Time Self-Assembly of Stereomicroscopically Visible Artificial Constructions in Incubated Specimens of mRNA Products Mainly from Pfizer and Moderna: A Comprehensive Longitudinal Study

Young Mi Lee, MD [1], Daniel Broudy, PhD [2]

[1] Practicing physician with a specialty in Obstetrics and Gynaecology, Hanna Women's Clinic, Doryeong-ro 7, KumSung Building, 2nd Floor, Jeju, Jejudo, 63098, Republic of Korea, Tel: +82-64-711-7717, email: youngmil95@gmail.com (ORCID: 0000-0002-1210-4726)

[2] Professor of Applied Linguistics, Okinawa Christian University, Nishihara-cho, Okinawa 903-0207, Japan, email: dbroudy@ocjc.ac.jp (ORCID: 0000-0003-2725-6914)

Abstract

Observable real-time injuries at the cellular level in recipients of the "safe and effective" COVID-19 injectables are documented here for the first time with the presentation of a comprehensive description and analysis of observed phenomena. The global administration of these often-mandated products from late 2020 triggered a plethora of independent research studies of the modified RNA injectable gene therapies, most notably those manufactured by Pfizer and Moderna. Analyses reported here consist of precise laboratory "bench science" aiming to understand why serious debilitating, prolonged injuries (and many deaths) occurred increasingly without any measurable protective effect from the aggressively, marketed products. The contents of COVID-19 injectables were examined under a stereomicroscope at up to 400X magnification. Carefully preserved specimens were cultured in a range of distinct media to observe immediate and long-term cause-and-effect relationships between the injectables and living cells under carefully controlled conditions. From such research, reasonable inferences can be drawn about observed injuries worldwide that have occurred since the injectables were pressed upon billions of individuals. In addition to cellular toxicity, our findings reveal numerous — on the order of 3~4 x 10^6 per milliliter of the injectable — visible artificial self-assembling entities ranging from about 1 to 100 μm, or greater, of many different shapes. There were animated worm-like entities, discs, chains, spirals, tubes, right-angle structures containing other artificial entities within them, and so forth. All these are exceedingly beyond any expected and acceptable levels of contamination of the COVID-19 injectables, and incubation studies revealed the progressive self-assembly of many artifactual structures. As time progressed during incubation, simple one- and two-dimensional structures over two or three weeks became more complex in shape and size developing into stereoscopically visible entities in three-dimensions. They resembled carbon nanotube filaments, ribbons, and tapes, some appearing as transparent, thin, flat membranes, and others as three-dimensional spirals, and beaded chains. Some of these seemed to appear and then disappear over time. Our observations suggest the presence of some kind of nanotechnology in the COVID-19 injectables.

Keywords: *mRNA, modified RNA, COVID-19 vaccine incubation, stereomicroscopic examination, nanotechnology*

Introduction

In the early days of the push to herd earth's population into the COVID-19 global "vaccine" experiment, a small number of medical doctors and independent researchers began raising concerns about the observed ineffectiveness, even negative impact, of the modified-RNA injectables (Beattie, 2021; Hughes, 2022; Santiago, 2022; Nyström and Hammarström, 2022). In addition to questions raised about their ingredients, their reported mode of defending the body focused on inducing serum-neutralizing antibody IgG production instead of generating more effective secretory antibodies (IgA). The latter in the respiratory mucosa have always served as the principal line of natural defense against viral respiratory infections. Given the possibility that new variants of SARS-CoV-2 could be rapidly induced by billions of injections being promoted by authorities worldwide, increasing numbers of deaths were attributed to strains of SARS-CoV-2 and severe sequelae (Lyons-Weiler, 2020; Vojdani & Kharrazian, 2020; Vojdani et al., 2021) leading to many deaths in population centers around the world (Beattie, 2021).

Official Korean Government reports as of December 2022, for example, showed approximately 2,600 deaths and more than 18,000 other acute sequelae from the COVID-19 injectables. The contradiction between claims of efficacy and material evidence of harm is inescapable: South Korea could claim one of the highest vaccination rates in the world (88% jabbed at least 3 times) while effectively, thereafter, also exhibiting the highest infection rate (89%) in April 2022 when flu season and respiratory colds are at a minimum. These facts alone are signs that the injectables provided no protection and were not preventing COVID-19. The reverse was the case. The injectables were neither safe nor effective. These figures alone should motivate physicians and medical researchers to reconsider the maxim that "correlation does not equal causation". In some instances, it does (Beattie, 2021, 2024). Here, we show observable real-time correlations between causes and effects in the living cells of human beings as they react to the toxicity of COVID-19 injectables. We also show microscopic evidence of self-assembling structures appearing in various media in which the fluid from COVID-19 injectables, particularly, Pfizer and Moderna products, were incubated for up to 12 months or more.

In the wake of the mass vaccination program, by as early as March 2021 and over the following months, significant increases in excess deaths of "unknown" causes and severe sequelae — blood clots, inexplicable haemorrhaging, multiple organ damage (and failure), sudden spikes (cardiotoxins) in heart disease, blood cancers including leukemia and lymphoma, a range of other "turbo" cancers, miscarriages, neurological and autoimmune disorders, to name a few, have appeared in patients (Nyström and Hammarström, 2022; Santiago & Oller, 2023; Perez et al., 2023; Mead et al., 2024a[1]).

These observations spurred our interest in examining the larger picture both in society and in the laboratory where clearer images of the injectable contents themselves could be subjected to careful analysis under the microscope. This report of our results was aided by the independent research of a cohort known as Korea Veritas Doctors (KoVeDoc) with whom we shared injectables manufactured by Pfizer, Moderna, AstraZeneca, and Novavax. All of these were widely used throughout South Korea. These products appeared to cause a range of negative health effects in patients: advanced stages of aggressive breast cancer, dysfunctional uterine bleeding, spontaneous abortion, sudden increases in heart disease (dyspnea and palpitations), pneumothorax disease, multiple skin diseases, and rapid onset of aggravated autoimmune conditions.

[1] Editor's note: The paper by Mead et al. (2024a) was retracted soon after the journal *Cureus* published it. Part 1 (Mead et al., 2024b) of the two part response to that unwarranted retraction has already appeared in *IJVTPR*, and Part 2 will soon follow (2024c).

Observational studies commenced on December 10, 2021. Preliminary analysis of the contents showed that the Pfizer and Moderna products were substantially different from the other COVID-19 injectables — AstraZeneca and Novavax. The differences, to be discussed throughout this report, motivated the initial work with the Pfizer and Moderna products, as the contents were prepared for analyses, and for later incubation in various culture media, we had in mind seeking out chemicals, protocols, and solutions that might prove to be suitable detoxifying agents in treating patients. Twelve months seemed, at the time, to be an adequate duration to begin to understand more clearly the longer-term effects of the products when they were injected into the human body and exposed to various ambient conditions, including electromagnetic fields and ultraviolet radiation.

Since drying the injectable COVID-19 fluids, as will be seen in our **Results** section, also produces more numerous and varied kinds of crystals, the apparent process of self-assembling entities can be camouflaged by certain naturally forming crystals, mainly salts, for instance. As we discuss below, drying out the incubated materials can easily introduce a bias which, we presently surmise, may have led certain other researchers to hastily claim that all of the observed self-assembling entities emerging from the nanotechnology (imperceptible with many ordinary microscopes), does exist in the COVID-19 injectables. The fact that such nanotechnology is in the COVID-19 injectables was first discussed, we believe, by Campra and colleagues (2021a, 2021b; Spectroscopy & Campra, 2021) . They used much more powerful spectroscopic methods and equipment revealing what appeared to be programmable entities at the nano-level. More recently, Diblasi and Sangorrin (2024) have confirmed and extended the results of Campra and colleagues. In view of their findings, and our own, which are presented in detail below, we can reject the hypothesis that the self-assembling entities you will see in our **Results** section consist of nothing more than naturally forming crystals, mostly salt or cholesterol as was suggested by Bigtree and Cole (2022).

Materials and Methods

Fifty-four samples were used in the study: 50 residual injectable vials (43 Pfizer, 7 Moderna) acquired immediately after their use in the COVID-19 vaccination campaign, and 4 unopened new injectable vials (2 Pfizer, 1 AstraZeneca, 1 Novavax). Initial observations were made on Pfizer and Moderna products under an Olympus stereomicroscope on the same day the vials were first used. Residual fluids in the vials were preserved at −20° Celsius in a laboratory freezer for subsequent study. Later, after thawing, the residual samples were placed in various culture media for long-term observation. The objective was to observe any changes that might occur over time and that might be observable under the microscope.

Injectable fluid samples as well as blood and semen specimens were examined under a stereomicroscope augmented with by a Makler Counting Chamber. Laboratory conditions were maintained with a stereomicroscope, a laminar air flow clean bench, a heat template, and an ultra-violet light as shown in **Error! Reference source not found.**.

The stereomicroscope is a highly specialized tool for examining 3-dimensional and dynamic specimens and it is also useful in observing the results of micro-procedures commonly applied in the context of assistive reproduction protocols — intracytoplasmic sperm injection, assisted hatching, blastomere biopsy, etc. The Makler Counting Chamber is also specialized for counting sperm cells in limited space for the evaluation of male fertility. All procedures were carried out

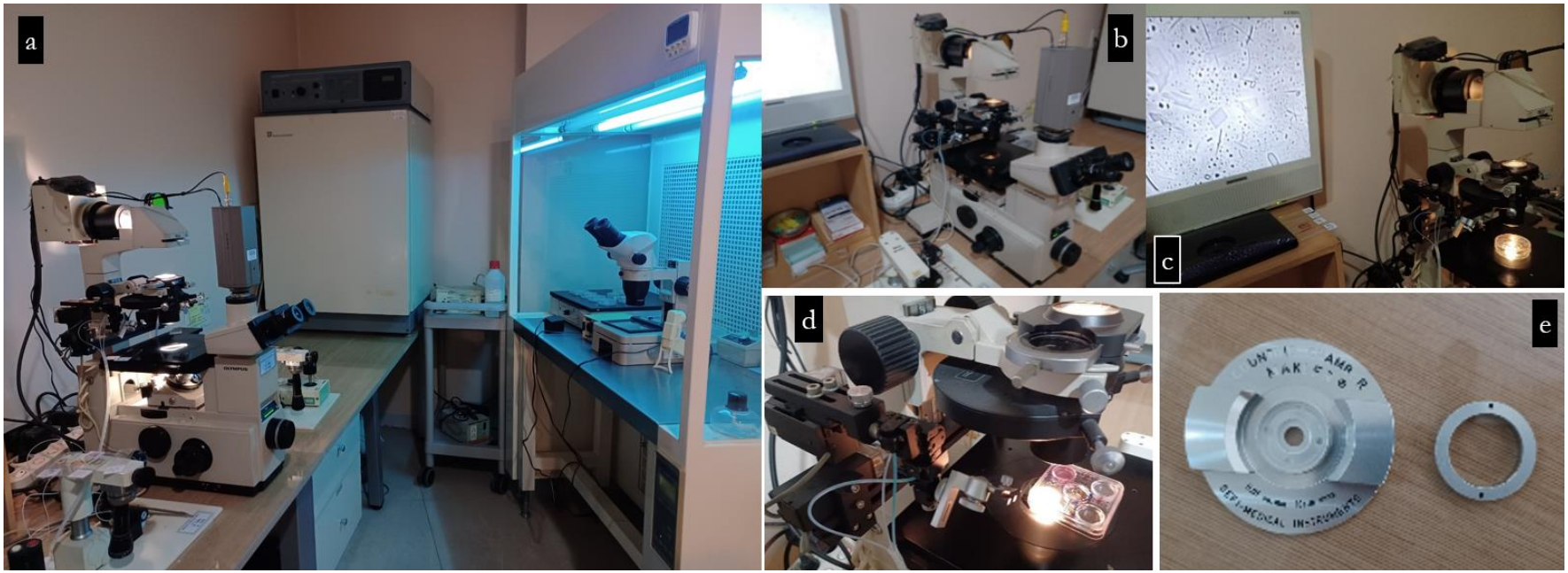

Figure 1. Lab equipment: (a) at right, a stereomicroscope, a laminar air flow clean bench with UV and heat template; (b) a stereomicroscope connected to an LCD monitor for viewing; (c) Moderna culture dish on the stereomicroscopic plate with video monitoring; (d) 5 well culture dishes on the plate; (e) a Makler Counting Chamber.

aseptically on a clean bench in the Hanna IVF [*In Vitro* Fertility] laboratory — registered No. 138 by the Korean Ministry of Health and Welfare as a specialized sterile space. Due to concern during the study period about possible cross-contamination of specimens, all procedures in fertility treatment were suspended. Due, also, to the additional concern about the unpredictable nature and potential behavior of exposed nanomaterials, the laboratory was permanently closed to any public access.

1. Direct Microscopic Examination of mRNA COVID-19 Injectables

Fifty-four COVID-19 injectables (both residual and new) as well as 1 flu vaccine and a separate sample of normal saline (both serving as controls) were examined with the stereomicroscope. Analysis included 45 vials of Pfizer (43 residuals, 2 new ones, 11 lot numbers) and 7 vials of Moderna (all residuals with 5 lot numbers), 1 new AstraZeneca, and 1 new Novavax.

The Makler chamber aided in an accurate method of counting unidentified floating materials in the various products.

All vials were preserved by refrigeration at −20° Celsius and were examined under the microscope after thawing at room temperature (RT) to approximate more closely the environment at sites where the injectables were administered — hospitals, clinics, and other health institutions. Because the study involved numerous data points, it was exceedingly difficult to control all the samples and associated lot numbers, so we offer Table 1 containing only the ones that were tracked and could be confirmed.

Table 1
Lot Numbers for the COVID 19 Injectables That Were Studied

COVID-19 Injectable	Pfizer (P1) for Adults	Pfizer (P2) for Children	Moderna (M)	AstraZeneca (AZ)	Novavax (NV)	Flu Vaxigriptetra Prefilled Syringe for Injection	0.9 Percent Sodium Chloride in Solution (Normal Saline)
Lot Number	FT1940	FP8290	2100653	CTMAV578	ND0222002	V3H13	Jeil † LOT 01619098
	FL4209		2100654				Huons BA1096
	FM3092		2100681				Huons BA1065
	FN5430		2100683				Daehan † LOT 05W9AF3
	FK0592						
	FT7280 for booster (P4)						

† Normal saline (Jeil & Daehan) was used a dilutant for Pfizer at 1:6. Dilutions were not needed for other injectables listed here.

2. Blood and Semen Reactions

Blood and semen samples were also examined for their exposure and potential reactions to all four COVID-19 injectables with the flu vaccine and normal saline (0.9% Sodium Chloride) being used as controls.

To rule out bias and possible confusion with blood potentially contaminated from injectable contents, a whole blood specimen was collected from a non-vaccinated participant and plasma was prepared from a supernatant layer via natural sedimentation for approximately 3 hours at room temperature to avoid any kind of mechanical damage from the centrifugation. In the interest of preserving natural coagulation mechanisms and avoiding unexpected biochemical intervention, for the purity of the samples (blood or plasma), this procedure did not use any EDTA-coated containers.

Eight separate glass slides were prepared for observation of how injectables interacted with blood samples. Each of the first four slides held one drop of whole blood and a micro drop of each injectable. The drops were positioned in a way that interaction could be easily achieved and observed with the use of cover slips which allowed for the progressive mixing of samples. Four plasma samples were, subsequently, treated for observation in the same way. In the interest of understanding interactions of the injectable materials in various media — blood plasma of non-injected persons, whole blood of such persons, semen samples from injected and non-injected males, and various other liquid media over time. Digital documentation of the changes in bodily fluids and living cells was accomplished by repeated video recordings over regular intervals from 5~10 minutes, 30 minutes, 1 hour, 2 hours, or more, and for studies involving just the injectable materials incubated in various fluids, the recordings varied from intervals of days to weeks and months as are reported in our **Results** section.

As ideal and easily interpretable representatives of living cells, via their recognizable motility even during short-term culture studies, semen samples provide an excellent basis for examining the progressive impact of cytotoxicity over time. With respect to the four semen specimens that we examined in detail, three samples were from vaccinated participants who had received 2 or 3 COVID-19 injections, and who later reported fertility problems and gave consent for using their earlier collected semen specimens for our experimental purposes, and one was from a person who had not received any COVID-19 injection. At the time when the semen samples were initially collected, none of the "vaccinated" donors had reported any negative "side effects" of the COVID-19 injections each of them had received. Before the experimental study, all semen specimens were categorized as normal, according to the World Health Organization with respect to sperm count, morphology, and motility (WHO, 2021). Significantly, the control sample from the "unvaccinated" individual was of excellent quality. The donor was relatively young, still in his twenties, and had not been exposed to whatever toxic effects the other three donors may have experienced because of being injected with a COVID-19 "vaccine". Supplementary fluids and other known or potentially toxic materials that we studied with respect to the motility of sperm samples included soju (Korean distilled spirits, 20 proof), red wine, beer, and silica water. Also, adding them to the normal saline solution (as a control) we examined the impact of Vitamin C, mica, and the incubation media of skin extracts taken from an injected recipient. We expected that the degree of cytotoxicity of any of the milieux examined would show up in the motility of the sperm cells from the various donors.

3. Incubation Study

In addition to the foregoing, multiple approaches to incubating the components of the various injectables were applied. This incubation aspect of the study was motivated by an effort to observe and draw reasonable inferences concerning the long-term effects of the COVID-19 products injected in 13.4 billion doses into 5.13 billion distinct human bodies as of April 8, 2024

(Pharmaceutical Technology, 2024). A minute sample (0.03ml) of each injectable product (Pfizer 1, 2, and 4, Moderna, AstraZeneca, and Novavax), was added to normal saline, sterile distilled water, and Hartmann's solution each contained in a separate culture dish (either a 1.2 ml for embryo culture dish, 5-welled culture dish, or an 8 ml for Petri dish) at room temperature (15~25 degrees Celsius, adjusted for seasonal changes) without any special added materials. Three kinds of culture dishes and a schematic of each culture dish can be seen in Figure . Because of the way each dish was covered and maintained in relatively sterile conditions, the possibility of outside contamination was minimal. Over the course of all the incubation studies run in parallel, there is strong evidence that none of the culture dishes were ever contaminated by any outside bacteria or fungal spores. However, foreign entities could be seen over the course of time as suggested in the side view of the hand-drawn illustration of a culture dish in Figure . One (1D) to three (3D)-dimensional entities could be seen developing on the flat bottom of the dish that would transform themselves over time into complex three-dimensional forms that seemed animate or at least able to float up through the fluid medium as suggested at the far right of the hand-drawn illustration in Figure .

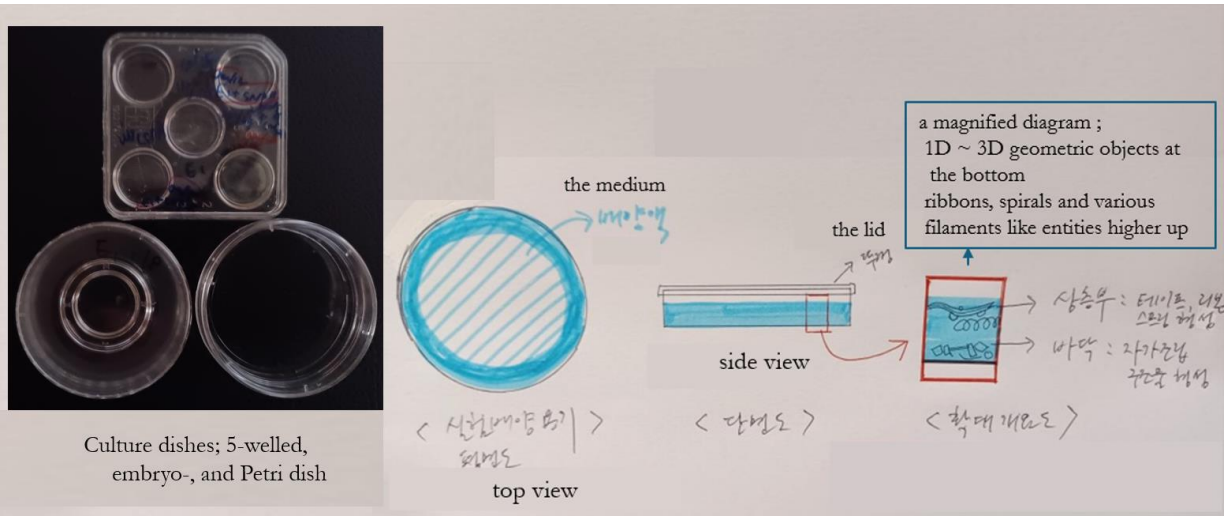

Figure 2. Various culture dishes with a hand-drawn schematics and notations in Korean and English to illustrate the setup and covering of cultures incubated over time: at the left are culture dishes seen from above; then reading left to right the top down view is contrasted with a side view showing the fluid inside covered with a transparent lid; and at the extreme right, an expanded side view depicts 1 to 3 dimensional geometric objects and floating filamentous structures as well as 3-dimensional geometric entities on the flat bottom of the dish whereas ribbons, spirals, and filamentous objects appear higher up swimming or floating in the fluid medium.

Three Pfizer products — designated here as P1 for adults, P2 for children, and P4 as a booster — as well as the Moderna COVID-19 injectable, were incubated in various solutions with certain chemicals and crystals added in order to observe their potentially therapeutic or detrimental effects. The chemical solutions that were used consisted of highly toxic chlorine dioxide (ClO_2), calcium hypochlorite ($Ca(OCl)_2$), and hydrogen peroxide (H_2O_2), which were carefully examined under controlled dose-dependent conditions, in other words, closely accounting for the proportions of the potentially therapeutic or detrimental components added into each solution.

The solutions containing added crystals included (1) various brands of colloidal silver and gold, mica (a Korean mineral complex), (2) EDTA (ethylenediaminetetraacetic acid, a chelator that readily attaches to iron and calcium, which is an aminopolycarboxylic acid with the formula $[CH_2N_2]_2$), (3) silica water, and (4) baking soda.

Blood plasma reactions were also studied with separate specimens taken from two non-vaccinees. Each consisted of the supernatant of the person's whole blood separated via natural sedimentation. The sample of blood was merely left standing for about 3 hours in a container to obtain the plasma after most of the blood cells accumulated in the lower part of the container. Subsequently, the two plasma samples were each incubated with small amounts of the Pfizer and Moderna injectables. Because there was a limited supply of each person's blood after one or two samples of plasma had been prepared, distilled water or normal saline was added to maintain their liquidity.

All the media were replenished weekly, or whenever necessary, to maintain sufficient consistency of liquid and to avoid total evaporation, which produces increased crystallization. We inferred from prior experience with natural crystals in various living media that drying out the fluids would camouflage any actual structures emerging from invisible nanomaterials contained in the fluids. With that idea in mind our approach was designed to enable us to tease out any self-assembling nanotechnology in the COVID-19 injectables by more intensive microscopy, and more rigorous laboratory bench science than had been applied previously. We suppose now, based on many hours of observation of samples from the injectables, that increasing salt crystallization in any medium by drying, would also tend to hamper the self-assembly of whatever invisible nanostructures may be contained in the injectables. There are, it seems clear now from our results (see below), self-assembling structures that begin as invisible nanomaterials in the fluid products that were incubated in various solutions. We will have more to say about those structures becoming visible through observable self-assembly as the incubated COVID-19 injectable fluids — especially the Pfizer and Moderna products — were observed over time for up to one year. Periodic examination under the stereomicroscope and recordings of observations were undertaken and saved in a digital format for later, more detailed, intensive, and recurrent examination.

4. Heat, EMF, 5G, and UV Light Study

a) Heat

Pfizer and Moderna samples were added to separate normal saline culture dishes and placed on a heat template set at normal body temperature, 36.5° Celsius, for 48 hours. Microscopic examination was carried out before and after exposure to heat.

b) Wireless Recharger with Mobile Phone

Pfizer and Moderna samples were used for this study in separate solutions of normal saline or distilled water, at about 101 incubation days for Pfizer and 36 days for Moderna. The culture dishes were situated atop a cellular phone in a wireless recharger, and they were set on 5G streaming mode for 1~2 hours. Electromagnetic field (EMF) measurements were taken through a Tri-phase measuring device (Figure) and were found to be 300v/m, 0 in H-field on the wireless recharger. The temperature was about 15~20 degrees Celsius.

c) External Hard Drive Exposure

Same incubation-staged dishes of Pfizer (day 101) and Moderna (day 36) samples in normal saline or distilled water were used and placed on an external hard drive for 2 hours to evaluate potential EMF effects. The external hard drive was connected to a PC and was activated when given various tasks in file management. Measurements taken on the surface were about 30v/m and 4μT in the hard-drive-field. The temperature was about 23°~25° Celsius.

d) UV Light Study

Samples were placed in separate dishes and exposed to ultraviolet light overnight. Before and after each experiment, microscopic examinations were undertaken, and video images were recorded and saved in a storage unit for later retrieval and detailed analysis.

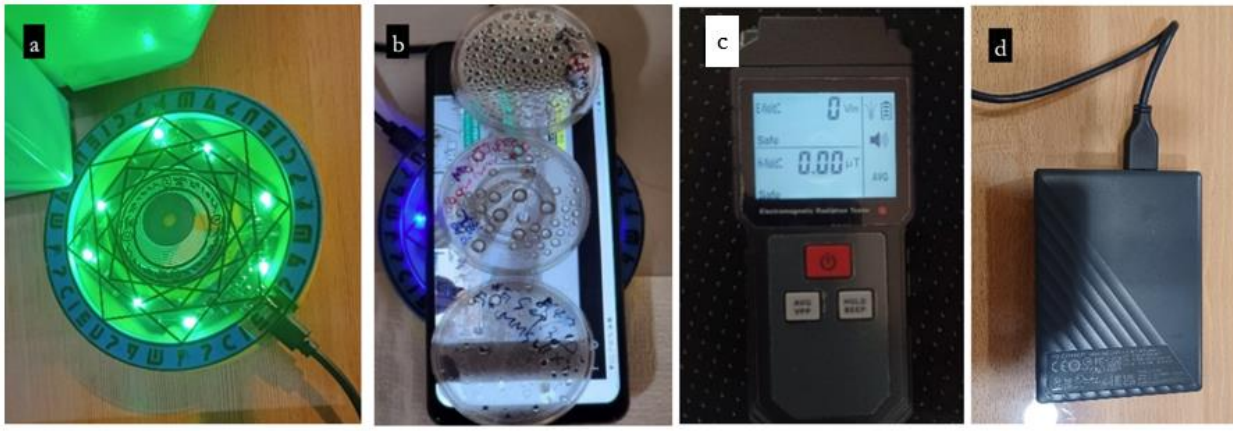

Figure 3. Electromagnetic field (EMF) equipment used: (a) a wireless recharger; (b) multiple culture dishes placed on the cellular phone; (c) the Triphase measuring device; and (d) the external hard drive for additional exposure.

5. Bio-Chemical Analysis of Injectable Culture Media

To isolate and understand the injectable components indirectly, biochemical screening tests were done with a urine stick (Abbot, UroCro4, U040H012A). To avoid possible contamination from culture media, each U-stick was exposed to 1 micro-drop of each injectable medium. The color change of each specimen was interpreted by the standard colorimeter.

6. Recycling Pattern

During the initial period of incubation, skin extracts (a variety of Morgellons) from an injected subject were placed in normal saline. The donor of the extracts was a patient suffering from the side effects of a paralytic seizure sustained just days after injection of the mRNA experimental product. Her specimens from the Moderna injectable were anonymized and coded as Extract 1 (E1). During the initial examination of the skin extract, surrounding particles appeared and seemed to exhibit a symbiotic relationship through direct observation under the stereomicroscope. After one month incubation of E1, enough seed-shaped particles, less than 1 μm in their largest dimension, sufficiently developed in size were observed floating and moving around the main portion of the skin extract in the saline solution of the culture dish. The particles were carefully collected and

incubated in different normal saline dishes for about 1 year or a little longer. Regular examination under the microscope of the changes in these particles over time was at first neglected because the researcher simply forgot to make the recordings. However, the incubation of the skin extracts was maintained in normal saline. After day 366, however, the researcher remembered this aspect of the ongoing studies and from then onward high-resolution images were examined, recorded, and preserved for subsequent detailed analysis.

Results

1. Direct Microscopic Examination

Injectables

Regarding normal saline as a control reference, at a magnification of 400X, no abnormal floating materials were ever observed (Figure a), but in 4 vials of Flu vaccine 2~3 floating particles were seen at the same high-powered magnification (Figure b), and 1 new vial of AstraZeneca and 1 new vial of Novavax showed 1~ 2 floating particles in the 1~3µm range under the same level of magnification (Figure c).

Figure 4. (a) Normal saline control compared against (b) flu vaccine and (c) AstraZeneca injectable at 400X magnification

Contrastingly, all residual and new vials of the Pfizer injectables (including 2 new ones, with 11 different lot numbers) revealed many unidentified variously shaped floating entities, about 2~100µm in their largest dimension. These freely moving particles were algorithmically counted and estimated to contain about at 3~4 x 10^6 such entities per millilitre. Of those entities, about 30% had a worm-like shape, in addition, there were also rods, discs, and crystal-like mixtures, but the various samples showed vial-to-vial differences in both the predominant shapes seen in them and in the density of those shapes (Figure 5a-left side portion). When the Pfizer samples were incubated at body temperature for up to 2 days, they showed more development, seemed to become active as if responding to a command to change into various other forms — additional worm-like mating pairs appeared, also hovering layered discs, spheres, and elongated tube-like objects (Figure 5a, see the right-hand side, D1 and D2). Compared to the Pfizer sample, all 7 vials of Moderna had a greater number of particles and, also, more artificial moving structures — discs, coils, beaded chains, and bunches of chandelier-like coils (Figure 5b, left half).

When the thawing and freezing process was repeated, there appeared an increase in unidentified floating materials and entities that seemed to have been notably activated (see Figure 5b, top frame showing changes with a repeated cycle of freezing and thawing). When the new original vial of Pfizer concentrate was examined under the stereomicroscope, it showed only a few moving worm-like entities or a few small particles, but contrastingly when it was diluted in a 1:6 ratio (0.3 ml : 1.8 ml) with normal saline following the recommended practice for injection into a human recipient, the contents appeared to wake up, come to life and get activate, revealing a profusion of various shapes

of rods, key-shaped structures, and other formations within a few minutes. These new entities did not resemble any known, natural, or identifiable organic entities (Figure 5b — new Pfizer).

All dried specimens of COVID-19 vaccines were studied under the stereomicroscope. The contents appeared as various geometric forms in the Pfizer and Moderna samples while Moderna exhibited more enlarged irregular geometric patterns. In contrast, AstraZeneca showed a few small discs in various sizes while Novavax showed notably fewer dark material entities, and not so much crystal formation (Figure 5b, see the right-hand side). The fact that thawing, refreezing, and thawing again would produce such changes might show at least one of the reasons the manufacturers would urge users to maintain the injectables at extreme freezing temperatures (− 70° Celsius with Pfizer).

2. Blood and Semen Reactions to the Injectables

Experiments were carried out to assess reactions of blood and semen under precisely controlled and observed conditions. We used normal saline and flu vaccine — VaxigripTetra in particular — for comparison to the injectables, in a double-control multiple-treatment design. The injectables (Pfizer, Moderna, AstraZeneca, and Novavax) were the distinct treatments. One of our main goals was to assess the cytotoxicity of the COVID-19 fluids when coming in direct contact with living cells.

To achieve this aim the COVID-19 micro-drop was carefully positioned on the glass slide where it could come into contact with a drop of plasma or whole blood so we could record the interactions across time. A single drop of whole blood, or plasma, was placed on the left portion of the slide while a single micro-drop of the injectable was placed on the right side. By pressure from the cover slip, the fluids would meet at the center of the slide where any interactions between them could be observed and recorded. The stereomicroscope offered an excellent view of the movement and mixture over regular intervals from 5~10 minutes, 30 minutes, 1 hour, 2 hours, and thereafter. All responses to the interactions were recorded in a dated and time-stamped series.

As previously noted, whole blood was collected from a vein in a non-vaccinated participant, and plasma was prepared by natural sedimentation. The COVID-19 injectables, Novavax, in particular, showed the most significant interaction: rapid and toxic effects on blood cells. Other injectables showed relatively less rapid toxicity, but similar detrimental effects also appeared in red blood cells, white blood cells, and platelets (Figure and Figure). The varied negative effects are compared for severity over time and across interacting samples in Tables 2 and 3.

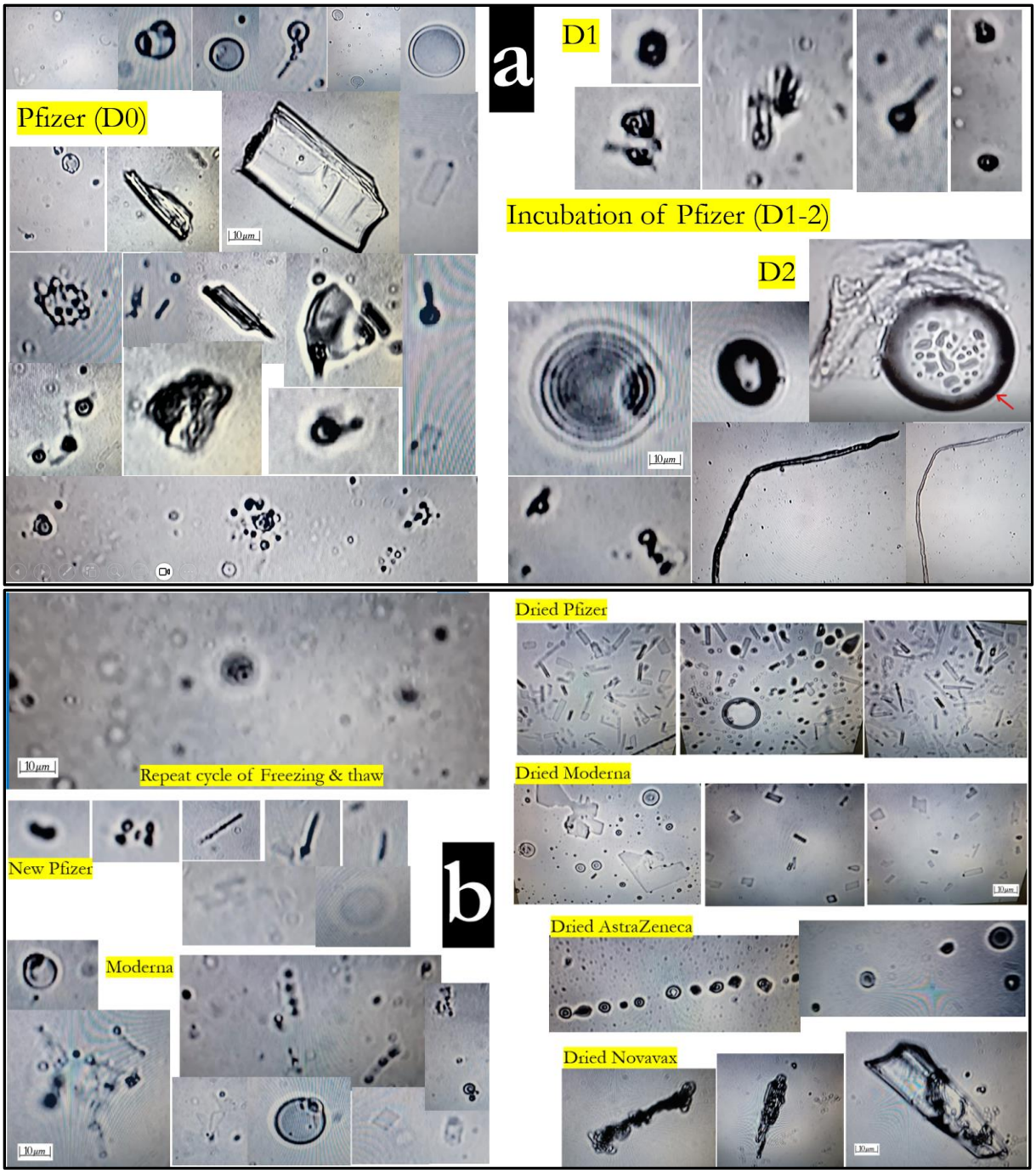

Figure 5. Direct microscopic findings observed in two dimensions magnified 400X: (a) Remnants and new Pfizer injectables, directly observed as well as after incubation for 1 -2 days. (b) Moderna and 4 dried COVID-19 injectables (Pfizer, Moderna, AstraZeneca, and Novavax).

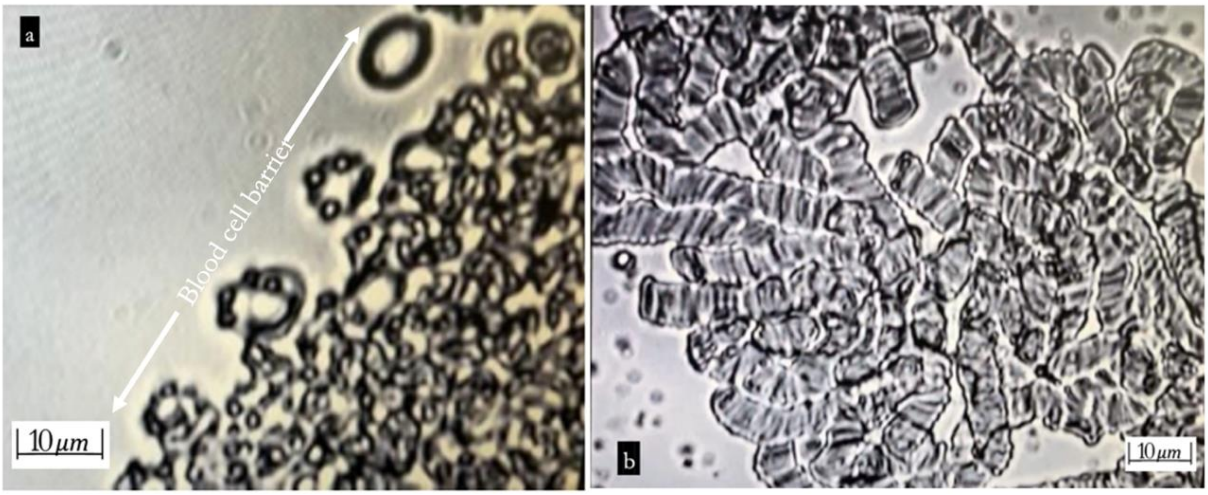

Figure 6. Interactions observed for whole blood(a)/plasma(b) with Novavax at 400X magnification: (a) Within 1 hour, blood cells formed a prominent barrier against "vaccine" contents. (b) After 30 minutes, severe aggregates of red blood cells in rouleaux appeared in the plasma specimen.

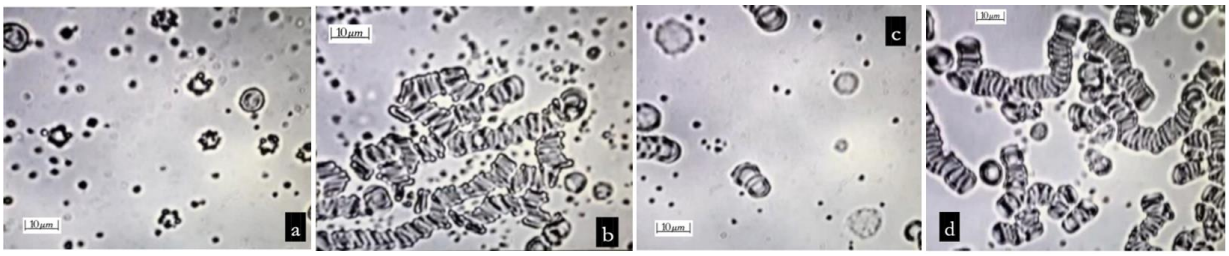

Figure 7. Plasma reactions after two hours with four COVID-19 injectables — Pfizer, Moderna, Novavax, and AstraZeneca: (a) Pfizer showing cellular collapse (pyknosis) of white blood cells and damaged platelets; (b) Moderna with stacks of red blood cells (rouleaux); (c) Novavax with the nucleus of white blood cells disintegrating (karyorrhexis), abnormal platelet aggregations, and some rouleaux of red blood cells; and (d) AstraZeneca with prominent Rouleau of red blood cells.

Noteworthy was the behavior of each kind of blood cell, mobilizing as though in a battle on a frontline moving against each of the injectables — red blood cells against Pfizer and AstraZeneca, white blood cells against Moderna, and platelets against Novavax. Despite their observed behavior, these injectable-specific phenomena could be related to their characteristic direct blood pathophysiology — blood flow stasis and following hypoxemia (fatigue) from the Rouleaux pattern, immune suppression from white blood cell damage, and blood clot formations (thrombosis) or bleeding tendencies from platelet damage or aggregation.

Semen studies were conducted with the same controlled methods applied in the studies of blood. Samples from three COVID-19 "vaccinated" donors and one "non-vaccinated" donor were examined as in the studies of blood. Results are summarized in Table 4.

Table 2
Whole Blood Reaction to the Various COVID-19 Injectables Listed

	Initially	After 1 hour
Pfizer	Red blood cells on the frontline against the vaccine White blood cells, some damaged, some not	Red blood cells — still on the frontline White blood cells damaged to a mild degree Platelets damaged to a moderate degree
Moderna	White blood cells on the frontline	Red blood cells on the frontline White blood cells collapsed in cytoplasm Platelets aggregating to a mild degree
AstraZeneca	Red blood cells on the frontline Spreading to the blood (intermingled with each other well)	Mixed well and beginning to form fibrin
Novavax	Platelets on the frontline	Established the clear border between "vaccine" and blood RBC withdrawal backward

Table 3
Plasma reaction to the various COVID-19 vaccines.

	Initially	After 30 min	After 2 hours
Pfizer	Red blood cells on the frontline	Red blood cells still on the frontline	White blood cells with pyknosis, Platelets damaged Red blood cells forming rouleaux to a mild degree
Moderna	Platelets aggregating Red blood cells forming rouleaux to a mild degree	White blood cells damaged Platelets aggregating	Red blood cells forming rouleaux to a moderate degree Platelets aggregating
AstraZeneca	Red blood cells forming rouleaux to a moderate degree Platelets aggregating	Red blood cells forming rouleaux to a severe degree Fibrin like formation	Red blood cells forming rouleaux to a moderate degree
Novavax	Platelets and white blood cells on the frontline Red blood cells forming rouleaux to a severe degree	Platelets on the frontline Red blood cells forming rouleaux to a very severe degree	White blood cells with notable karyorrhexis occurring and Red blood cells damaged and forming rouleaux to a severe degree

Table 4
Semen Response to COVID-19 Injectables Measured by Percent (%) of Motility

	Pfizer (P1, 2, & 4)				Moderna			AstraZeneca			Novavax			Flu Vaccine Control			Normal Saline Control		
	10m	30m	1h	2~3h<	10m	30m	1h<	10m	30m	1h<	10m	30m	1h	10m	30m	1h<	10m	30m	1h<
Semen 1 from a 47-year-old	10%	5%	1%	0%	10%	1%	0.1%	20%	1%	0%	5%	1%	0%	70%	60%	50%	70%	70%	70%
Semen 2 from a 44-year-old	P2 40%		P2 20%	P1 2h 30% 3h 20% P2 1.5h 5%		30%	0 %			2h 70% 5.5h 30%		10%	2h 1~ 5%		60%		70%		2h 60%
Semen 3 from a 38-year-old				P4 2h; 50% 41h † 1%			40%			30%									30%
Semen 4 28-year-old, non-vaccinee (control)	90%	P1 80% P2 70%		3h P1 80% very active P2 50%	80%	80%	3h 60%	70%	70%	3h 70%	80%	70%	3h 50%	80%	70%	3h 60%			50%

† = maximum lifespan**; m = min; h = hour**
Semen 4 exhibited the best quality at 12 x 10^6 sperm cells per millilitre with 80% motility.

Progressive death to sperm cells occurred within a few hours after exposure, even in low concentrations, to the various injectables. This rapid destruction of sperm cells did not align with our initial expectations, but the process was consistent with reactions observed in the blood specimens where we also saw less rapid but also progressive damage. As with the blood studies, Novavax showed the most significant toxicity in contact with sperm cells. They were rapidly immobilized and soon dead. While AstraZeneca showed mixed results in its impact on sperm specimens, Pfizer and Moderna were consistent in causing progressive lethal effects on each sample of semen. Normal saline or flu vaccine led to the expected natural degradation that would occur over time without any notable addition of toxicity. Motility was usually maintained for only a few hours. While 24 hours was the longest duration of survival for the sperm cells from a young and healthy donor who had not received any COVID-19 injectable, an exceptional and rare finding emerged.

Sperm cells from two recipients jabbed with Pfizer and incubated with Pfizer, survived for 41 hours. Could it be that the sperm cells from these two men who had received the Pfizer injectable, had been screened for susceptibility to injury by its contents? Perhaps the sperm cells vulnerable to destruction by the Pfizer injectable had already died off. However, our thought is that the longevity of the cells is related to their innate health starting out. That is, the response and vitality of sperm cells to the injectables depend more upon their quality than on any particular exposure. Nevertheless, all the COVID-19 injectables showed consistently lethal impact on some sperm cells within a few minutes or hours. Moreover, while AstraZeneca and Novavax are not mRNA-based, they also exhibited very serious and direct lethal effects on sperm and blood cells. Although the methods by which spike protein production differs in AstraZeneca and Novavax contrasted with Pfizer and Moderna, the recombinant spike protein contained already in Novavax seemed especially toxic to living cells. Summaries of the results we saw under the microscope are provided in Figure .

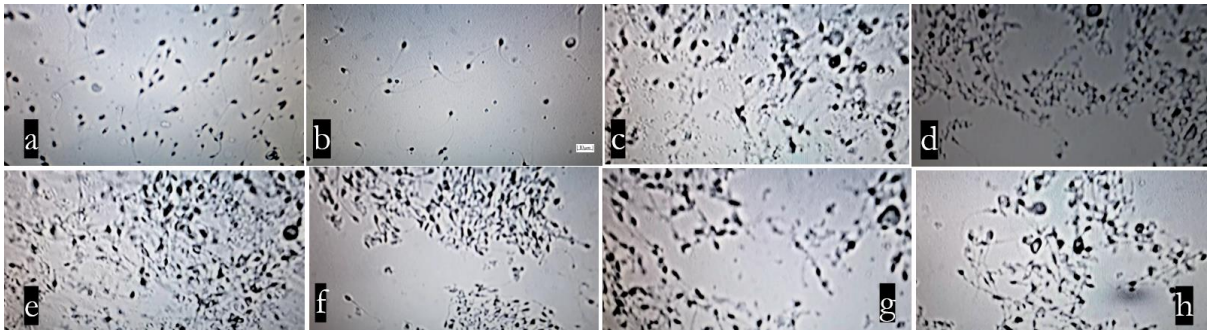

Figure 8. Reaction of semen to COVID-19 injectables at 200X magnification: (a) semen with normal saline as a control added after two hours; (b) with flu vaccine added as a control after 1.5 hours showed sperm cells with intact morphology and with typical progressive natural reduction in sperm motility; (c) 30 minutes after Pfizer-1 injectable was added, sperm motility showed rapid reduction; (d) Pfizer-1 after one hour, all sperm motility ceased; (e) 30 minutes after Moderna. injectable added; (f) one hour after Moderna was added sperm cells were completely immotile; (g) 30 minutes after Novavax was added; (h) one hour after Novavax, all motility ceased.

In sum, COVID-19 injectables have direct cytotoxic effects on living cells, especially on blood cells — red blood cells, white blood cells, and platelets — and on sperm cells. In addition to these observed interactions, additional harmful effects to living cells and the systems of the body are

almost certain to be occurring as well. The normal balances and homeostasis of pH, osmolarity, temperature, electrolytes in various concentrations, are all apt to be impacted by damage occurring at the cellular level. While there was variability across the samples, specimens from the vaccinated participants consistently showed immediate and/or progressive detrimental effects directly attributable to — observable while they were occurring because of — contact with the injectable materials. There were differences across the brands studied, but all of them caused observable damage attributable to toxicity. Perhaps the most interesting contrast observed was the fact that the sperm cells of the unvaccinated participant seemed to be damaged less than in semen from individuals who had received one or more of the COVID-19 injectables. The possible reasons for this observed resistance in control S4 (details in Table 4) could be linked to the participant's youth and health.

Results of comparative studies of semen and blood media from the incubated injectables are presented in Table 5 (see Appendix A). In tables (5, 7, 8, 9, 10, and 11), plus (+) signifies the presence of unspecified foreign structures while minus (-) signifies the clear absence. The degree to which these structures are observable is signified by two (++), three (+++), or four plus (++++) signs. The observation of questionable (or ambiguous) structures is signified by a plus and minus (+/-). The degree to which foreign structures are scarcely discernible is signified by a plus and two to four minus signs (+/--) (+/---) (+/----) with the latter being the most ambiguous in morphology.

While semen (S3) was taken from two jabbed recipients and while Plasma 1 and 2 are from individuals who were not vaccinated, the incubation study shows a more apparent trend in the development of filaments, ribbons, and chip-like structures in the semen than in the plasmas. We are not aware, however, of the precise cause of the difference between the semen sample and the plasma media. Despite this, in both samples, it appeared that the COVID-19 injectables could produce pre-programmed, self-assembling structures though in lesser quantity in the sperm from the unvaccinated individual.

Cytotoxic effects on semen from exposure to various popular supplementary materials or liquors (such as red wine, beer, and Korean spirits — 20 proof), vitamin C, mica, silica water, colloidal gold (GNP1), 0.001% (consumable standard concentration for the disinfection of the drinkable water) Calcium hypochlorite ($Ca(OCl)_2$) were examined. We also incubated skin extracts from E1 (the anonymous participant mentioned earlier) in normal saline solution over several months. The results were as follows:

Most solutions seemed to be directly toxic to sperm cells. They lost motility and almost all died within a few minutes up to 1.5 hours for the youngest and healthiest unvaccinated donor. Mica showed the lowest level of toxicity. Some sperm cells retained motility and were still alive (about 10% of them) up to 1.5 hours after exposure. In the most extreme case observed, some sperm cells, about 0.1%, for the young healthy donor, were still moving after a 3-hour time lapse. Korean spirits, more than other potentially toxic chemical observed over time, registered the most immediate direct and lethal toxic effect as seen in Table 6 (see Appendix A).

There is an important limitation on the foregoing results with live cells. Our design involves a kind of *in vitro* laboratory exposure, or incubation. Such exposures are only remotely comparable to fluids introduced *in vivo* to living human beings by injecting them into muscle tissue. Blood cells and sperm cells may be impacted by progressive fluid transport over minutes and hours depending on the relative efficiency of the cardiovascular and lymphoid systems of the individual. Transport can be

expected to be superior in younger and healthier persons — potentially making them more, not less, susceptible than older persons with less efficient fluid transport systems — to the sort of cellular damage our results demonstrate to be occurring *in vitro.* In some cases, nanoparticles, or other unidentified materials, could enter the bloodstream, cross the blood-brain barrier in both sexes, the testicular blood barrier in males, and the ovarian and placental barriers in females, directly impacting fertility and fetal health, but such contact presumably not could not occur in such a concentrated form as we studied experimentally.

Bearing these facts in mind, our experimental findings are certainly indicative of some of the consequences to be expected as the COVID-19 injectable fluids are carried throughout the body by natural cardiovascular and lymphoidal transport. To better understand the real effects in the human body, every attempt was made to recreate stable long-term incubation rather than short-term examinations. Our objective was to examine diluted and scattered impacts in ways that would be more comparable, presumably, to those occurring in living persons impacted by the injectables.

3. Incubation Study for the Injectables:

1) General Summary of the Incubation of the Injectables

Throughout the entire incubation period, which exceeded one year, no signs of bacterial or fungal contamination were observed in any of the mRNA vaccine specimens (Pfizer and Moderna). This is noteworthy because we did not rely on periodic exposure to any of the typical antibiotics or antifungal agents that are common to basic incubation studies. Because we were persuaded from direct microscopic observations in an earlier short-term incubation study (not presented here) that these foreign materials are not organic, but rather at least synthetic hybrid organisms or possibly animate robotic structures, we adopted an atypical approach to incubation. Our approach differs from usual culture methods, which periodically supply laboratory agents such as antibiotics and antifungal agents, or other antibacterial or antifungal disinfectants, that can dramatically alter the purity of the materials under observation. Growth, in our studies, was also maintained in small containers, but without any added O_2, or CO_2 supply.

Normal saline and distilled water were chosen as basic incubation media. These were ideal for the development of microscopically discernible foreign structures. For purposes of comparison, other specific electrolyte solutions (i.e. Hartmann's solution, 0.001% (1X) calcium hypochlorite ($Ca(OCl_2)$, 3% hydrogen peroxide (H_2O_2), and 1ppm (1/100 X) chlorine dioxide (ClO_2) were also used as incubation media. The latter media were less accommodating, according to our results, in triggering and enabling the self-assembly of foreign materials than were normal saline and distilled water. They possibly acted to suppress the development of self-assembling synthetic entities.

AstraZeneca and Novavax did not develop any self-assembled structures at the bottom of the dish, by contrast with the mRNA injectables from Pfizer and Moderna. While filaments in the upper layer seemed to occur very rarely, the source of their development remained questionable. Over long-term incubation, AstraZeneca and Novavax became contaminated with fungus and bacteria. That never happened with the mRNA cultures studies of Pfizer and Moderna. Pfizer and Moderna vaccines exhibited unique and consistent growth patterns. Figure 9 shows the peak stage of geometric patterns of self-assembly over two to six months in the COVID-19 mRNA injectable in various media whereas Figure 10 reports the various forms that developed progressively and maintained their structural integrity right up to the time of this writing.

Pfizer and Moderna injectables exhibited unique and consistent growth patterns. Figure 9 shows the peak stage of the artefactual (completely unnatural) sharp-edged geometric patterns that self-assembled over two to six months from the Pfizer and Moderna COVID-19 mRNA injectables in the various media at the bottom of the culture dishes. Figure 10 reports the various floating forms that developed progressively in the middle or upper layer of the culture dishes and maintained their structural integrity up to the time of this writing.

Over the first few weeks, various geometric structures self-assembled at the bottom of the dish.

> Week 1: 1 dimensional, rod-like entities or 2 dimensional simple flat rectangular shaped structures appeared.
>
> Weeks 2 ~ 3: 2 to 3-dimensional structures seemed to be added to the existing entities at the bottom.
>
> From day 14, well-made 3-dimensional structures were dislodged from the original frame at the bottom and rose into the upper layer (fluid layer depth about 6 ~ 8 mm). See Figure 2.

In Figures 11-19, we report the results of the incubation studies of the mRNA injectables for the whole period of observation. Of special interest are the self-assembling structures, presumably made from nanomaterials that were not visible under our power of magnification. We were limited to a maximum of 400X magnification. However, amazing self-assembling structures of great diversity became visible by about the fifth week of incubation. They consisted ultimately of ribbons, coils, and filament-like structures. They formed up and moved into the mid- and upper layers of the culture media containing fluids with Pfizer and Moderna from day 37 forward.

Regarding the self-assembled structures in the bottom layer (as shown in Figure 9), the peak stage of full assembly was presumed to be around 2~6 months of incubation. After this period, a progressive disintegration of the structures was observed, and the structures finally disappeared, except for a remnant trace. In their encapsulated circular form, perhaps the shape of these remnants signified some sort of dormant stage of development, as one might expect to observe in the pupa stage of a developing parasite (Figure 11 — k, l, m, and Figure 19 — j, k, l).

Interestingly, in the sterile distilled water, Pfizer samples exhibited more developed spirals (coils), tapes, filaments, membranes, beaded chains, which appeared to float in the middle layer just above the bottom or uppermost layer. This seemed to happen after their peak growth stage over the last few months of observation (Figures 12, 13, and 14).

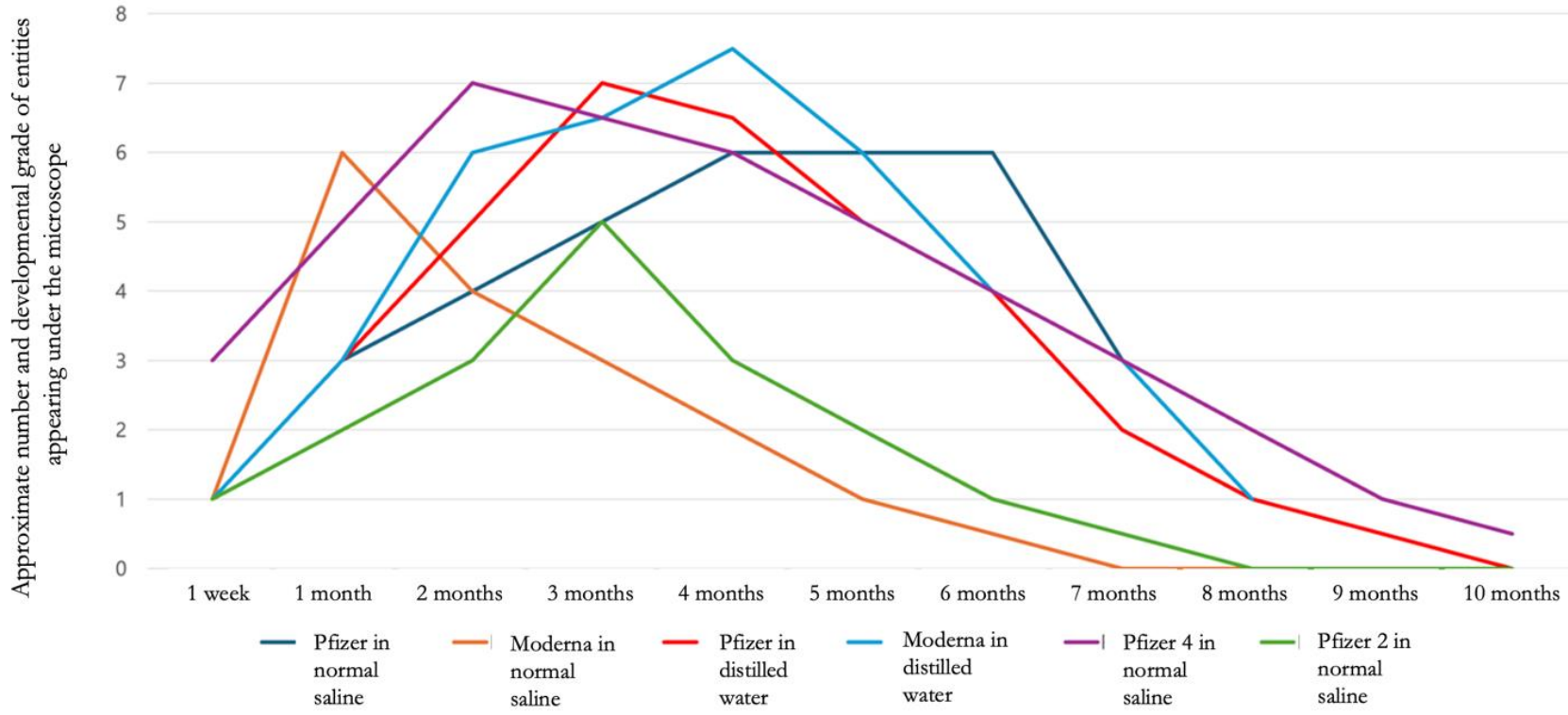

Figure 9. A visual summary of the emergence and development of various geometric entities appearing over a ten-month period of incubation of Pfizer and Moderna COVID-19 injectables: The developmental trend illustrated in the graph shows that 2 ~ 6 months of the incubation period is the peak stage for geometric self-assembly at the bottom of the culture dish irrespective of the kinds of mRNA vaccine and their culture media. After the peak stage of development, the assembled chip-like structures progressively disappeared.

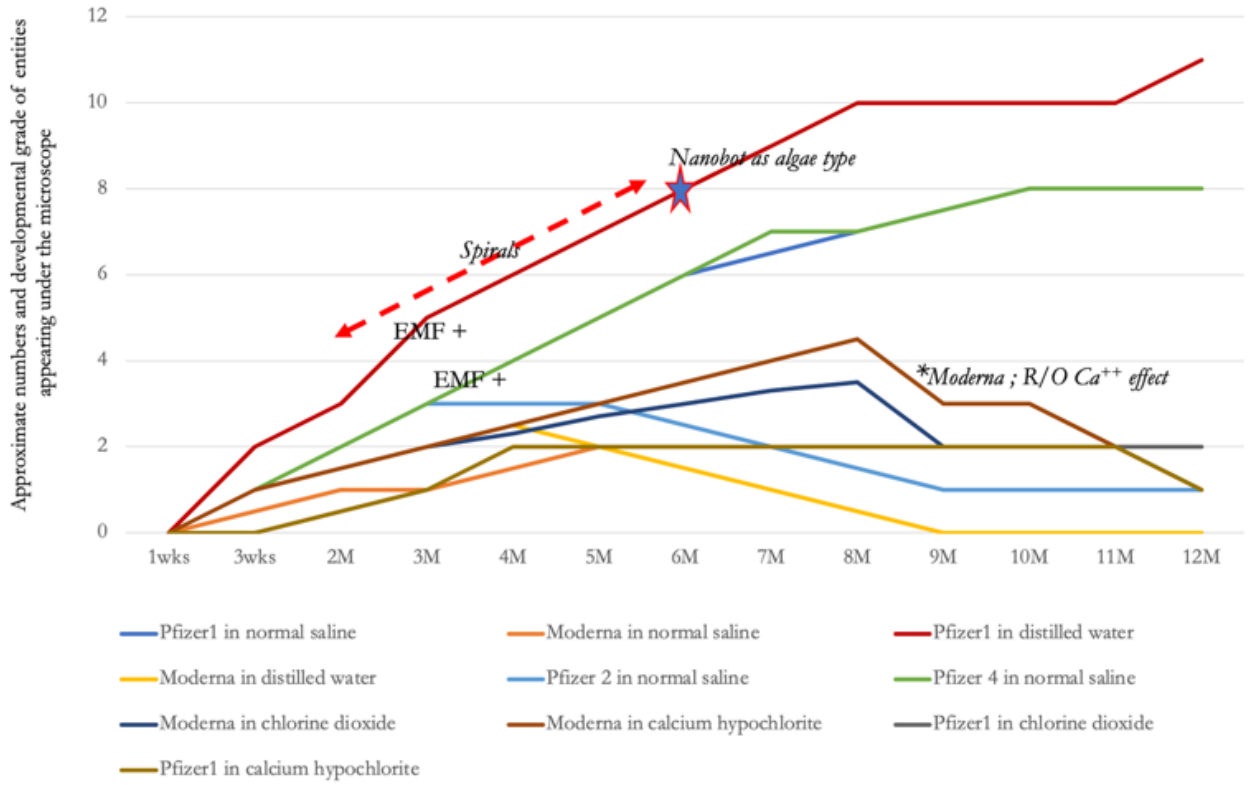

Figure 10. Growth pattern of floating structures — ribbons, spirals, filaments in the COVID-19 mRNA vaccines in the various media and electromagnetic field exposure throughout long-term incubation study: The graph shows that ribbons or spirals, and other various filaments, progressively appear and develop until the late stage of incubation, especially in distilled water and normal saline. Various spirals appeared transiently during 2 ~ 6 months of incubation, especially in distilled water. A magnetic nanobot-like structure ✪ appeared at about 180 days incubation and disappeared later in distilled water. An electromagnetic field from a wireless recharger appeared especially to stimulate the Pfizer sample to develop filaments both profuse in number and with lasting structural integrity in distilled water and normal saline. Pfizer 2 for children, not exposed to an electromagnetic field, is originally more diluted than Pfizer 1 for adults, so the developmental trend appeared to mimic that of Moderna. While Moderna did not produce profuse filamentous structures compared to Pfizer, Moderna did show relatively more filamentous structures and ones that were more sustainable in calcium hypochlorite. This phenomenon seemed to be mildly stimulated by Ca++ electrolyte.

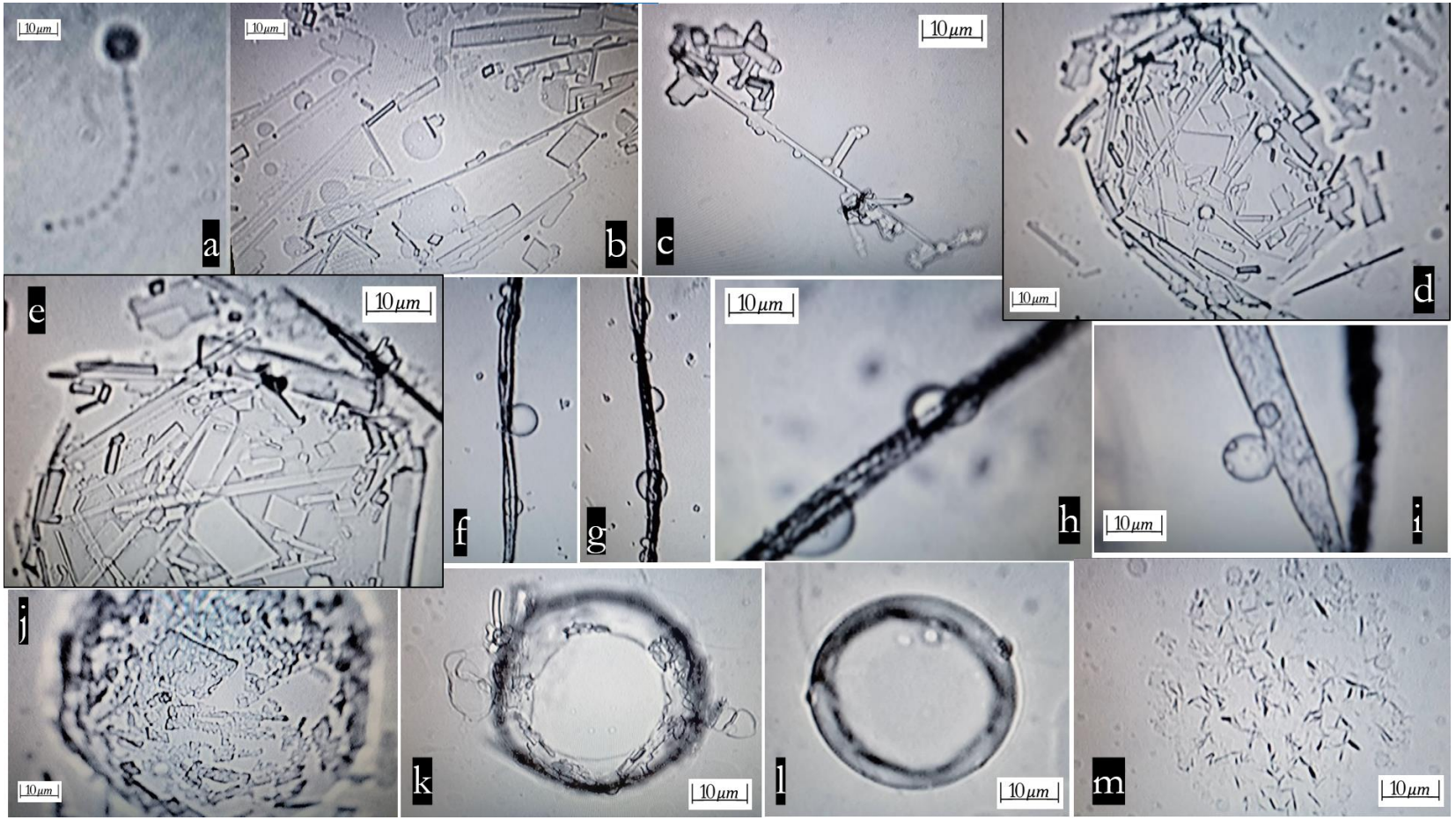

Figure 11. Findings for Pfizer incubation study for 372 days; (a) Day 22, this is what we describe as a beaded chain (at 400X magnification); (b) Day 24, 2-dimensional geometric self-assembly at the bottom (at 200X magnification) in normal saline; (c) Day 60, floating 3-dimensional detailed chip-like structures (at 400X magnification) in distilled water; (d) and (e) day 60, accumulated 3-dimensional chip-like structures within an oval shaped boundary (200X/400X) in distilled water; (f), (g), (h), (i) Floating filaments shedding bubbles inside and outside in normal solution at day 95 (100x/100x/200x/200x); (j), (k), (l), (m) Progressive degenerative changes in distilled water 200X (day 82/day 256/day 306/day 372).

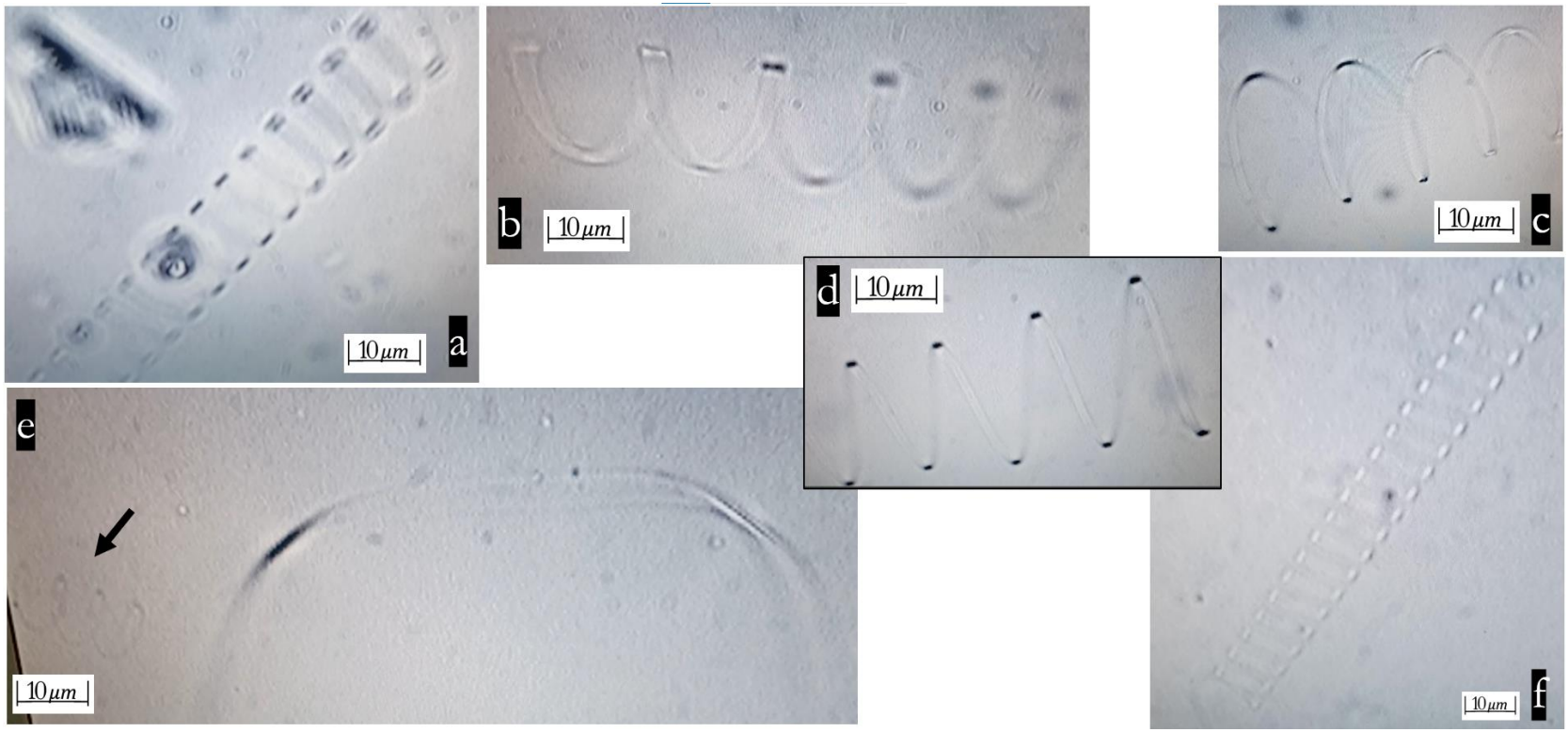

Figure 12. Various coils, ribbons, and spirals in Pfizer, distilled water: (a) Day 60 (at 200Xmagnification); (b) ~ (e) Day 74 (at 200X magnification); (f) Day 176 (at 100X magnification).

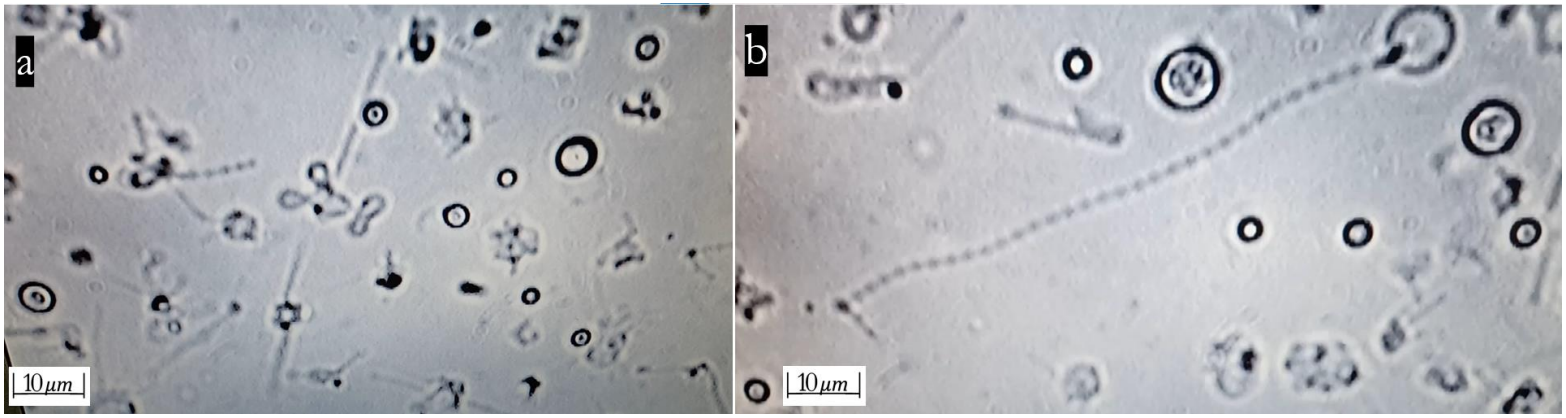

Figure 13. Beaded Chains and Assorted Structures in Pfizer Distilled Water (Day 176, 400x): (a) Various artificial satellite-like structures, (b) Long beaded chains gathered on the central surface of the medium.

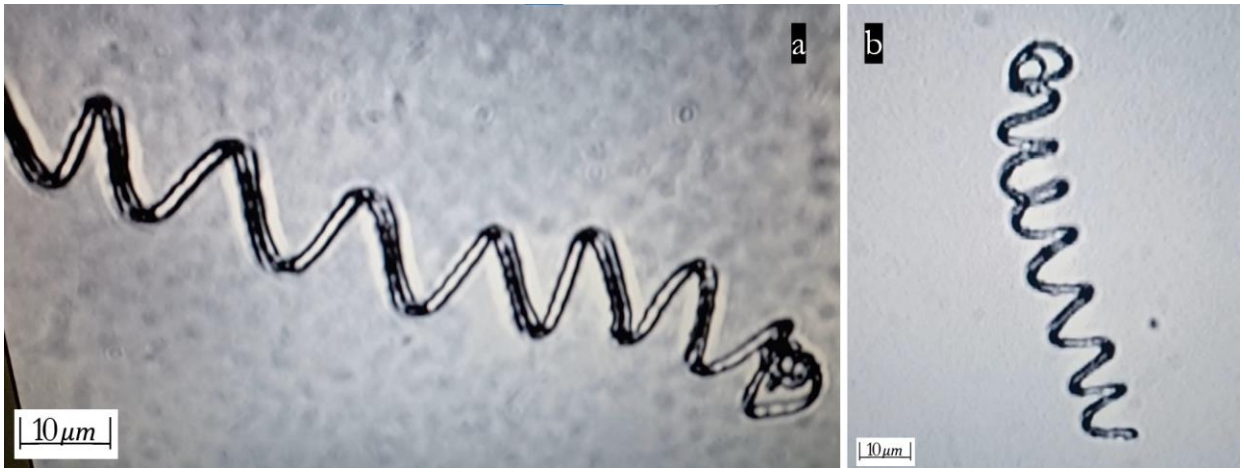

Figure 14. Typical Algae-typed Magnetic Nanobot-like Spirals in Pfizer in distilled water: (a) Day 176 (400x); (b) Day 337 (200x).

In what seemed to be the peak stage of developmental activity, the injectable samples had to be resupplied more frequently with water to keep them from dying out. This was especially so during the summer season when the formations described above seemed most active. Nearing the latter part of what we are describing as the stage of peak activity — after approximately 150 ~ 180 incubation days — specific algae-type magnetic bio-nano-robot like coils, dark irregular spirals, appeared near the bottom of the medium (Figure 14).

After this period, these kinds of structures continued to maintain their shape until about day 366 (and have continued as of this writing) in the Pfizer incubation studies, showing slightly denatured filaments sprouting out. Some of these filaments take the appearance of hollow bundles of tubes branching outward (Figures 15 and 16).

Floating filaments, especially in the Pfizer sample in distilled water, transformed into a few branching figures and, then, morphed again into hollow transparent elongated ribbons or thin tubes just as in images of participant E2 developing from her skin extracts. (Skin extracts from a Moderna vaccinee will be presented in a forthcoming paper) at day 337 during incubation.

In the final stage, at about day 337, familiar-looking filaments appeared in the middle layer of the Pfizer sample in distilled water. Depending on the materials, some floated near the bottom of the medium, others in the middle. Transparent wire-like bundles of hollow tubes appeared floating on the surface of the medium just as skin extract 2 (E2) appeared and changed to a tripod-like tipped filament (like the form of an anchor for connection to a neuron) or curled striated ribbons shedding bubbles. See Figures 15, 16, 17, and 18 for details.

The structures in the Moderna sample appeared to develop more rapidly than those in the Pfizer sample, (perhaps because Moderna included a higher concentration of particles). In the same way, the Moderna structures also disappeared more rapidly. In normal saline with Moderna, self-assembling structures appeared at the bottom layer with more artificial and chip-like figures emerging more rapidly and profusely, but with less developed filaments and coils (Figure 19).

During the peak stage of 3-dimensional geometric growth (2 ~ 6 months), we noticed that the incubation media, consistent with previous observations, became progressively turbid, exhibiting an emulsion-like appearance. After achieving this state, the media across all culture dishes began returning to their initial transparent state even as the presence of floating filamentous structures remained obvious.

In the late stage of Moderna incubation (day 630) in distilled water, nanoparticles reappeared floating again as previously seen during initial microscopic observations before culturing had commenced. This reappearance suggests a recycling pattern we describe later in a proposed model at Figure 27. While Moderna showed just a few filamentous structures with unique split ends and a few bundles of loose thin transparent nanowires, Pfizer, in contrast, showed very few nanoparticles floating in close proximity to the filaments or ribbons, but in a background largely cleared of surrounding nano-debris.

Figure 15. Various filaments — striated ribbons, sprouting in the late stage (day 316) of incubation of pfizer in distilled water: (a) and (b) curing striated ribbons (100x); (c) sprouting filaments in Pfizer (200x).

.

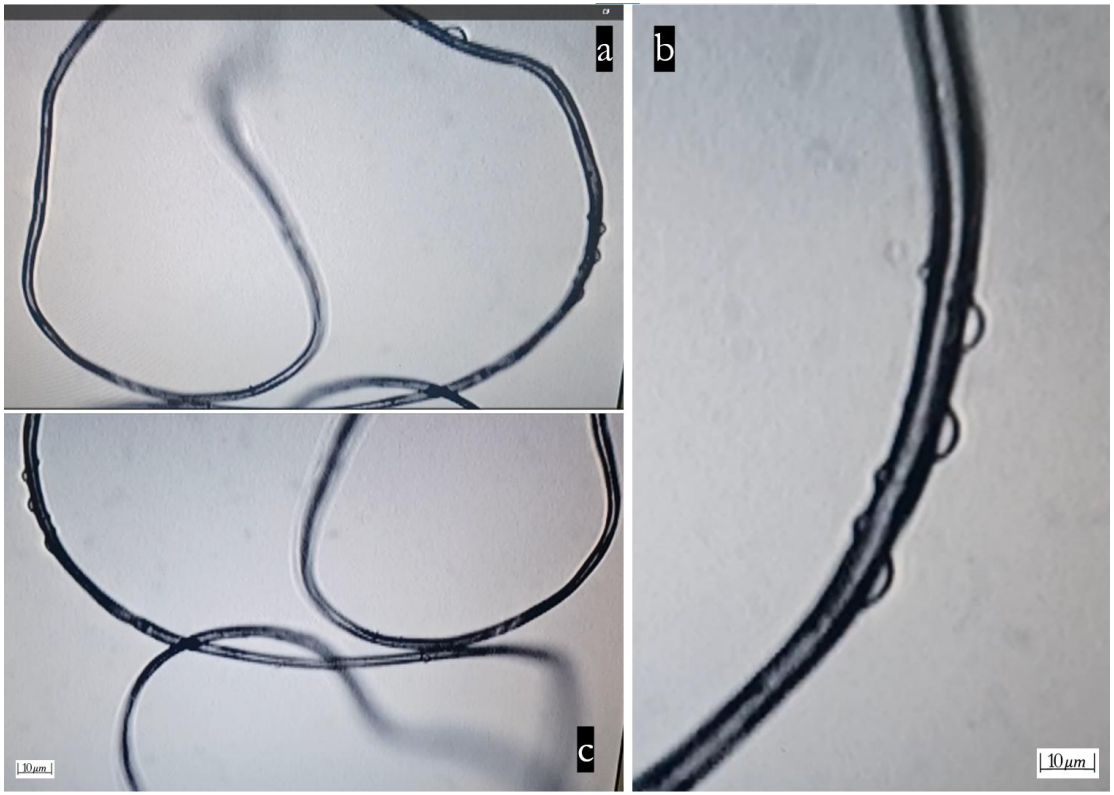

Figure 16. Bundle of transparent thin wire-like tubes with shedding bubbles in Pfizer incubation in distilled water (Day 331); floating in the uppermost layer (a-40x/b-100x/c-40x).

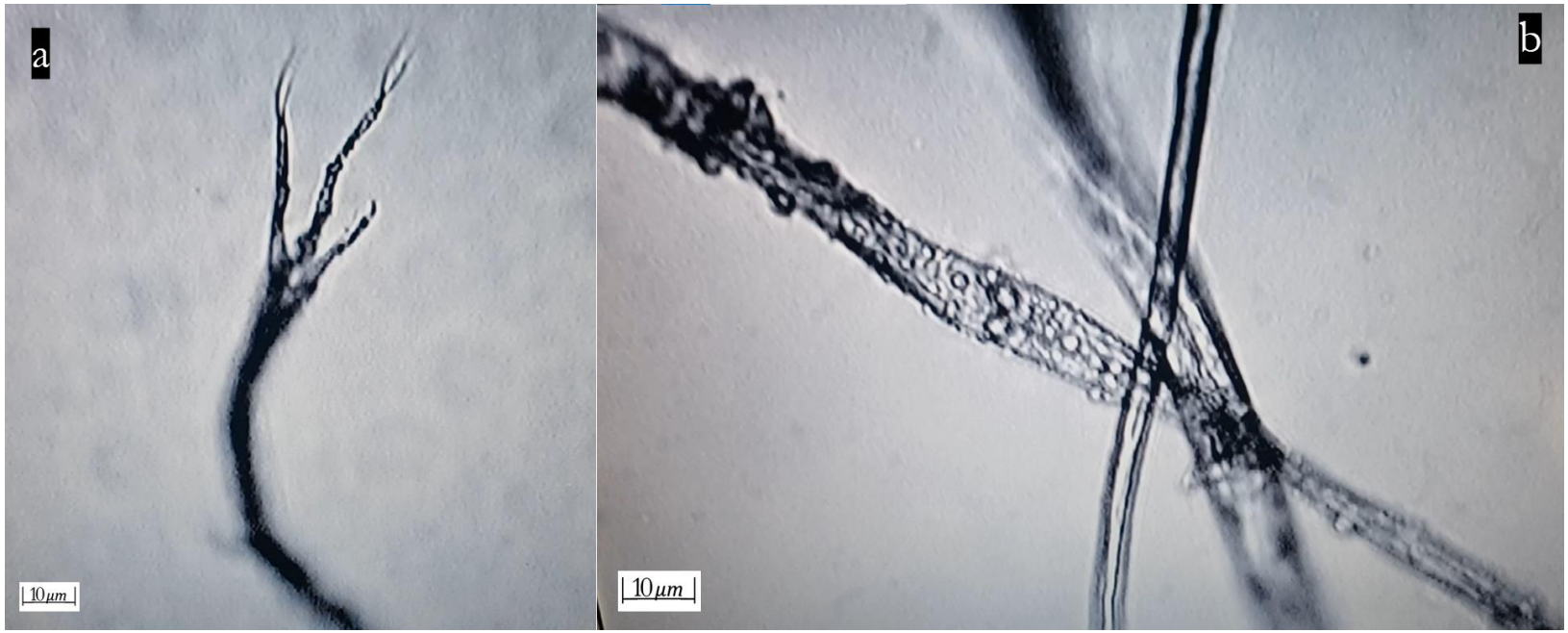

Figure 17. Tripod-like, striated filaments in Pfizer incubation in normal saline (D346, 200x): (a) More developed tripod-like structures or (b) Striated patterns on filaments.

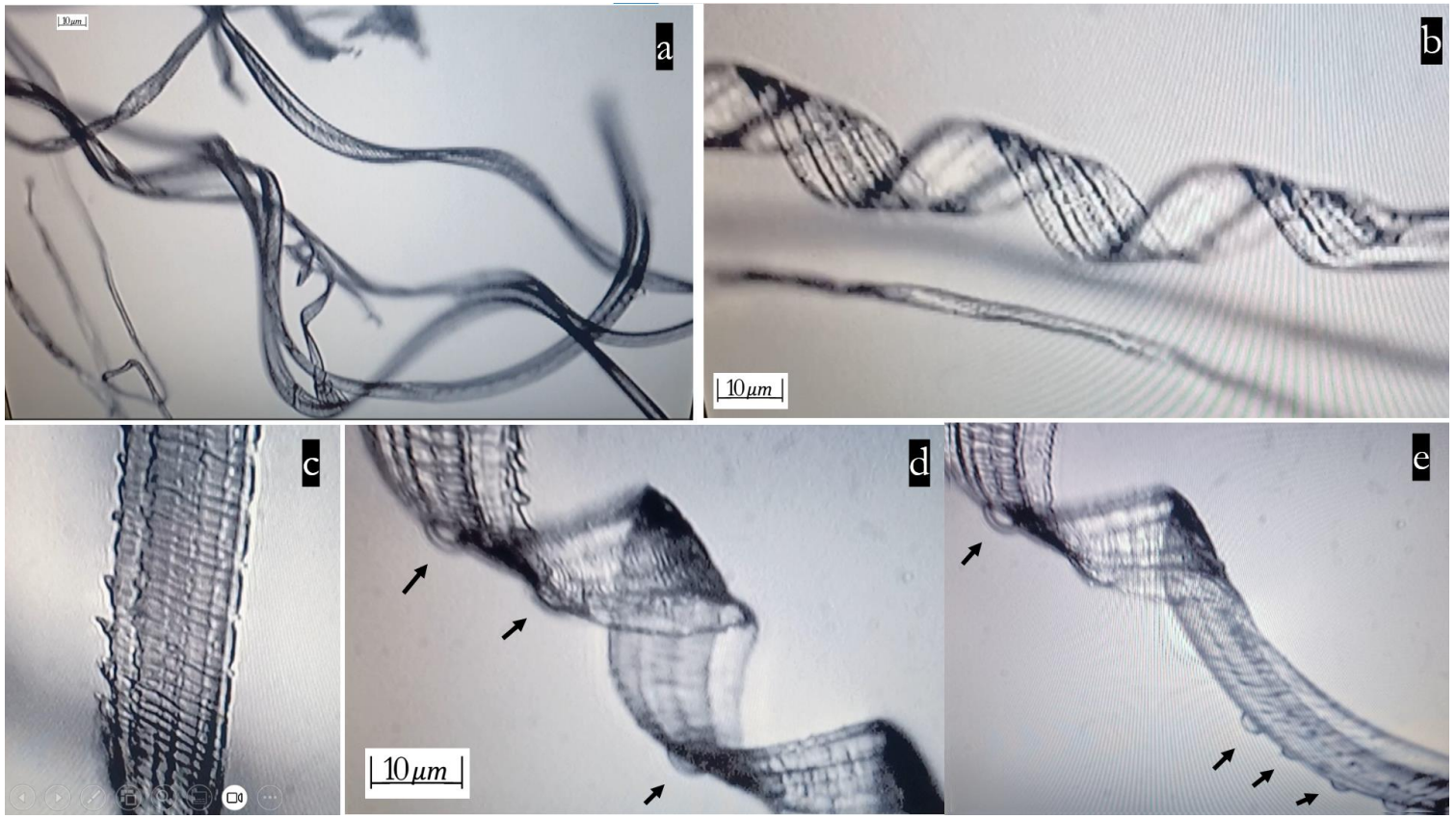

Figure18. Curled Striated Ribbons and Bubbles in Pfizer Incubation in Distilled Water (Day 406 and 499); (a), (b), and (c) uniquely striated curled Ribbons in Pfizer in DW at 406 days of incubation (40X/100X/200X); (d), and (e); Bubbles (arrows) appeared on the surface of the curled ribbons at 499 days incubation (200X).

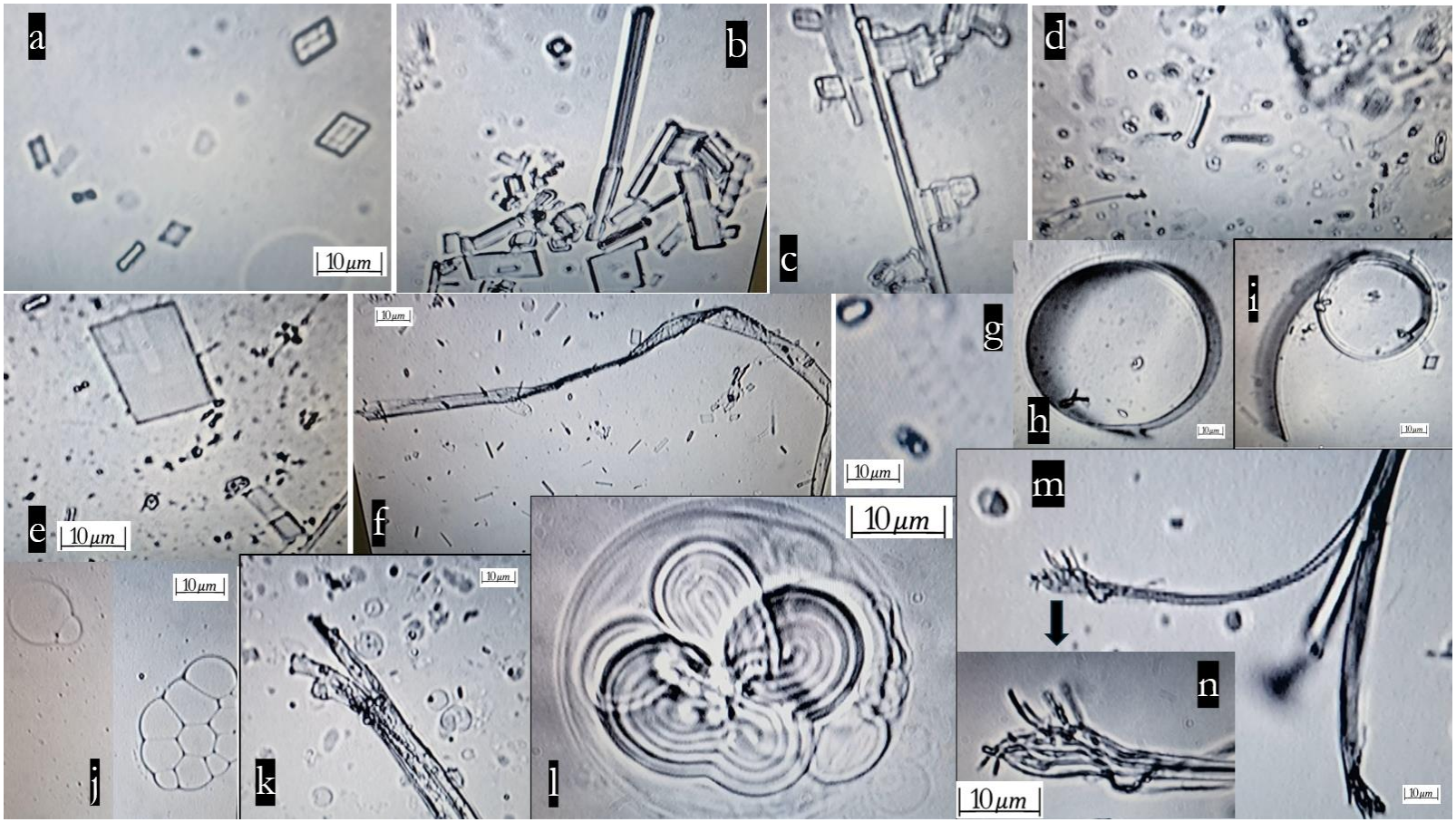

Figure 19. Geometric chip-like assembly, filaments, spirals, ribbons, and encapsulated wire bundles in the Moderna incubation study throughout Day 630 (100~400X): (a) Day 16; (b) Day 40; (c) Day 42; (d) Day 125; and (e) Day 126 (all 400x) in normal saline. (f) Day 126, chips and filament (100x) in normal saline; (g) Day 36, rarely observed small spring in distilled water; (h) and (i) Day 42, small circular ribbons in normal saline, (400x/200x); (j) Day 295, lobulated bubbles floating at the uppermost layer(100x) in distilled water; (k) Day 313, split-ended tape (200x) in distilled water; (l) Day 313, capsuled, well-packed wire bundles (400x) in distilled water; (m) Day 630, split-ended filament in normal saline (100x); (n) Day 630, magnified split-ended filament (400x).

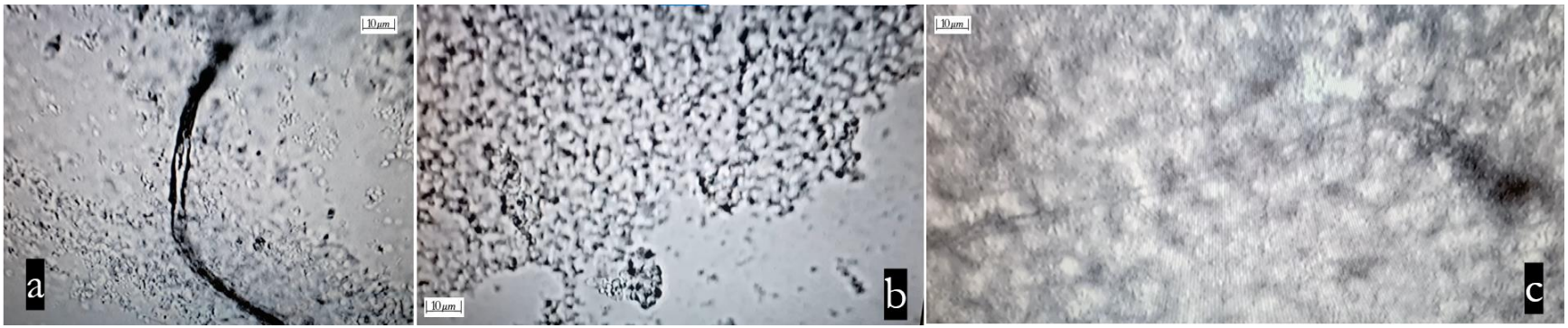

Figure 20. Pfizer and Moderna incubation study in plasma 1 and 2 (100x): (a) Pfizer in plasma 2 for 133 days (100x) — shorter filaments developed; (b) Pfizer in plasma 1 for 146 days (100x) — nothing found except blood cells; (c) Moderna in the plasma1 for 146 days (100x) — shorter thin trace of the filaments only.

During the late stage of Pfizer incubation (day 630), irrespective of the kind of media (either normal saline or distilled water), the injectable showed a greater proliferation of filamentous structures than did Moderna, including distinctly curled ribbons also in a clearer background.

In summary, the incubation study yielded tangible results. Various geometric chip-like structures self-assembled over the first two weeks of incubation, and more complex 3-dimensional structures emerged and dislodged from their templates at the bottom of the culture dish and migrated into the upper layer. Obvious signs of distinct sharp-edged geometric shapes as well as curvilinear shapes were evident. After approximately a month, floating structures then appeared and continued developing in the form of filaments, spirals, beaded chains, satellite structures, and ribbons. This study, beyond confirming the presence of undeclared unnatural foreign ingredients in the injectables, may encourage researchers to test whether a direct cause-and-effect relationship can be confirmed in the appearance of self-assembly at the bottom of the dish and the patterns of development of these diverse floating structures. We tentatively suspect from our observations that such a relationship is self-evident.

2) Developmental Changes in Various Media

Normal saline (N/S) and distilled water (D/W) were chosen as basic incubation media. These two media formed ideal conditions for the development of microscopically discernible foreign structures as described earlier in the 'Results' section.

In the distilled water, both injectables showed the widest variation of figures and materials — transparent spirals, ribbons, spiraled tapes, elongated bubbly filaments, etc.

For purposes of comparison, other specific electrolyte solutions (i.e. Hartmann's solution, 0.001%(1X) calcium hypochlorite ($Ca(OCl_2$), 0.03%(1/100 X) hydrogen peroxide(H_2O_2), and 1ppm(1/100 X) chlorine dioxide (ClO_2) also served as incubation media to investigate their possible detoxifying or aggravating effects. While these were less triggering to the self-assembly process of foreign materials in the early incubation stage, these solutions possibly acted to suppress the development of structures. However, in 0.001%(1X) calcium hypochlorite ($Ca(OCl_2$) and 1ppm(1/100 X) chlorine dioxide (ClO_2) in the middle stage (day 111) of their incubation with Pfizer and Moderna, chip-like self-assembly were progressed similarly to other basic incubation media solutions and finally produced a few and shorter filaments, too.

At the bottom of the Hartmann solution medium (as a plasma volume preservative medically), interestingly, in contrast to our expectations of increased development in an electrolyte-profuse solution, both Pfizer and Moderna showed less distinctly developed self-assembled structures, which appeared blunt-edged and irregular in shape. Except for a remnant of filaments that remained, these irregular structures finally disappeared in a process of progressive disassembly. Replication of this study would benefit from the addition of Hartmann's solution rather than normal saline or distilled water as a basic medical infusion fluid as we described earlier. A results summary appears in Table 7.

In the Calcium hypochlorite, $Ca(OCl)_2$ dose-dependent study, starting from the standard concentration (1X, 0.001%) for drinkable water, in a lower concentration, more developed filaments emerged. During the initial stage of observation, self-assembled structures did appear but progressively disintegrated more rapidly than in normal saline, perhaps due to disturbance from the electrolytes (disturbed by EMF within the dish environment) (Table 8 in Appendix A).

Interestingly, in the initial incubation stage of the Chlorine hydroxide (ClO_2) dose-dependent study starting from the toxic concentrate, 100ppm (1X) used for disinfection of medical instruments, similar, but less assembled structures formed but more appeared to float rather than set up at the bottom, as was typical in the other electrolyte media. This difference might be explained by the crystalline components of ClO_2 which could hamper the process of structural self-assembly. Generally, in the lower concentration (lower than 1/16~1/32 x), self-assembled structures developed progressively, but more floating filaments developed in the higher concentration (higher than 1/16 ~ 1/32 x). Finally, in the stronger and more toxic concentration of 1~1/2 x, self-assembly was not observed nor were floating structures present in the initial stage.

However, during the late stage of incubation in a low concentration (1/400 ~ 1/200x), chips were still rarely found at the bottom by day 230, but in a higher concentration, non-self-assembled structures were found at the bottom except crystals peculiar to ClO_2. A greater number of chips were found in the Moderna than in the Pfizer sample in the lower concentration (lower than 1/200x). Filaments were found at the later stage of incubation in the lower concentration, but no structures were found in a higher concentration (higher than 1/16x). Pfizer showed more filaments than Moderna in the lower concentration (lower than 1/16x) (Table 9 in Appendix A).

In 3% Hydrogen peroxide, H_2O_2 solution, some significant effects on the injectable via peroxidase in its contents were expected. The results, however, did not meet our expectations. In the initial stage of incubation, there were no observable dose-dependent differences as chips appeared well-developed, but less than in normal saline. The Moderna sample developed more structures with more discernible features than those in Pfizer in the various concentrations of H_2O_2 solution. Even in day 203 incubation with Moderna, 3-dimensional structures, such as chips, were rarely present at the bottom in 1/200x while 1~2 dimensional structures were found in 1/200x concentration. Filaments were found, but rare and relatively shorter in the Pfizer sample with 1/500x of H_2O_2 solution for 203 days incubation. There were still 1~2 dimensional traces of chip-like structures at the bottom, but nothing in 1/200x, weak remnants of 1-dimensional structures only contrasting from in the Moderna (Table 10 in Appendix A).

As we report above, through each dose-dependent study, these three solutions, when used in lower concentrations, did not show any definitive potential for recovery to stasis from nano-contaminations since, in higher concentrations, they are toxic.

3) Various Mineral Solutions:

Pfizer and Moderna injectable were incubated with Si water, 3 kinds of colloidal gold (GNP2 unknown, GNP3 at 5nm in 10ppm, and GNP4 at 5nm in 240ppm) 1 kind of colloidal silver (SNP, of unknown size and concentration), EDTA (chelating agent), Mica (Korean traditional mineral complex), and Myrrh for about 300 days. The results are summarized in Table 11 (Appendix A).

Significantly, Pfizer in the silica solution, showed less development of self-assembled chips than it did in other solutions. Moderna also showed progressively less development of chips in the silica solution. As regards the development of filaments, neither sample showed any prominent differences in reactions to Si solution. Therefore, doses of silica water appear to have the potential to disturb, to some degree, the initial self-assembly process of nanomaterials.

Interestingly, even in the late incubation stage, day 258, self-assembled 2-dimensional structures were sustained at the bottom of some culture dishes, especially in Pfizer and Moderna with colloidal gold 2 (GNP2) and Pfizer incubated in silica water.

In the colloidal silver and mica, bacterial or fungal contamination developed progressively. This development suggested that the intended engineered effect (artificial antifungal antibacterial effect) was diminished progressively by these kinds of minerals, not aseptic ones for oral route only. In the EDTA solution, the self-assembly process in the bottom layer was not significantly disturbed as filaments finally began to appear prominently and profusely in the Moderna sample during the 253 days incubation. While any direct detoxifying effects of EDTA on the injectable-induced artificial polymers *in vitro* remain unclear, the indirect benefits of EDTA *in vivo*, however, could be realized through the chelating effect.

As regards the potential for myrrh to detoxify, the material proved inadequate as a medium for observational study because of its turbidity and rapid solidification. The only observable action during the early stage of incubation was the formation of bubbles during the process of desiccation. It remains unclear whether myrrh contains potential detoxifying effects.

In the high alkaline solution of baking soda (pH 9), Pfizer could not develop any kind of assembly and filaments until 5-months incubation (not shown here in the above table).

4) Plasma Reactions:

This study involved observation of reactions to two kinds of plasma taken from non-vaccinees, collected from the supernatant of the whole blood via natural sedimentation (the standing process for about 3 hours in a container), and incubating them with small amounts of the injectables, Pfizer and Moderna.

Early on, the injectables began developing self-assembled structures (1 ~ 2 dimensions) among the profuse blood cells at the bottom of the dish over the initial 7 days, but only traces of self-assembly remained until 27 days incubation. It is plausible that a profuse quantity of blood cells — red blood cells (RBC)s, white blood cells (WBC), and platelets — already at the bottom of the culture could have disturbed the injectable assembly process, and finally negated their construction in a way that caused the materials to vanish. However, quite significantly, floating filaments or hose- or pipe-like structures began progressively emerging during the late stage of observational studies at 131 ~ 146 days incubation. Especially evident were dark pipe-like and lasso-like structures in the Moderna sample incubated in plasma samples 1 and 2. These structures appeared together with ordinary filaments, but not in the Pfizer culture dishes. Neither at the bottom nor in the upper layer of the incubated Pfizer sample in plasma 1 for 131 days did structures appear, except for only a remnant of blood cells. Since no structures had developed in the plasma 1 sample, the tentative explanation might be that some sort of plasma may possess positive attributes in mounting a natural immunological defense against self-assembly processes. Further tests would likely draw out a more definitive conclusion. See details in Figures 20 and 21.

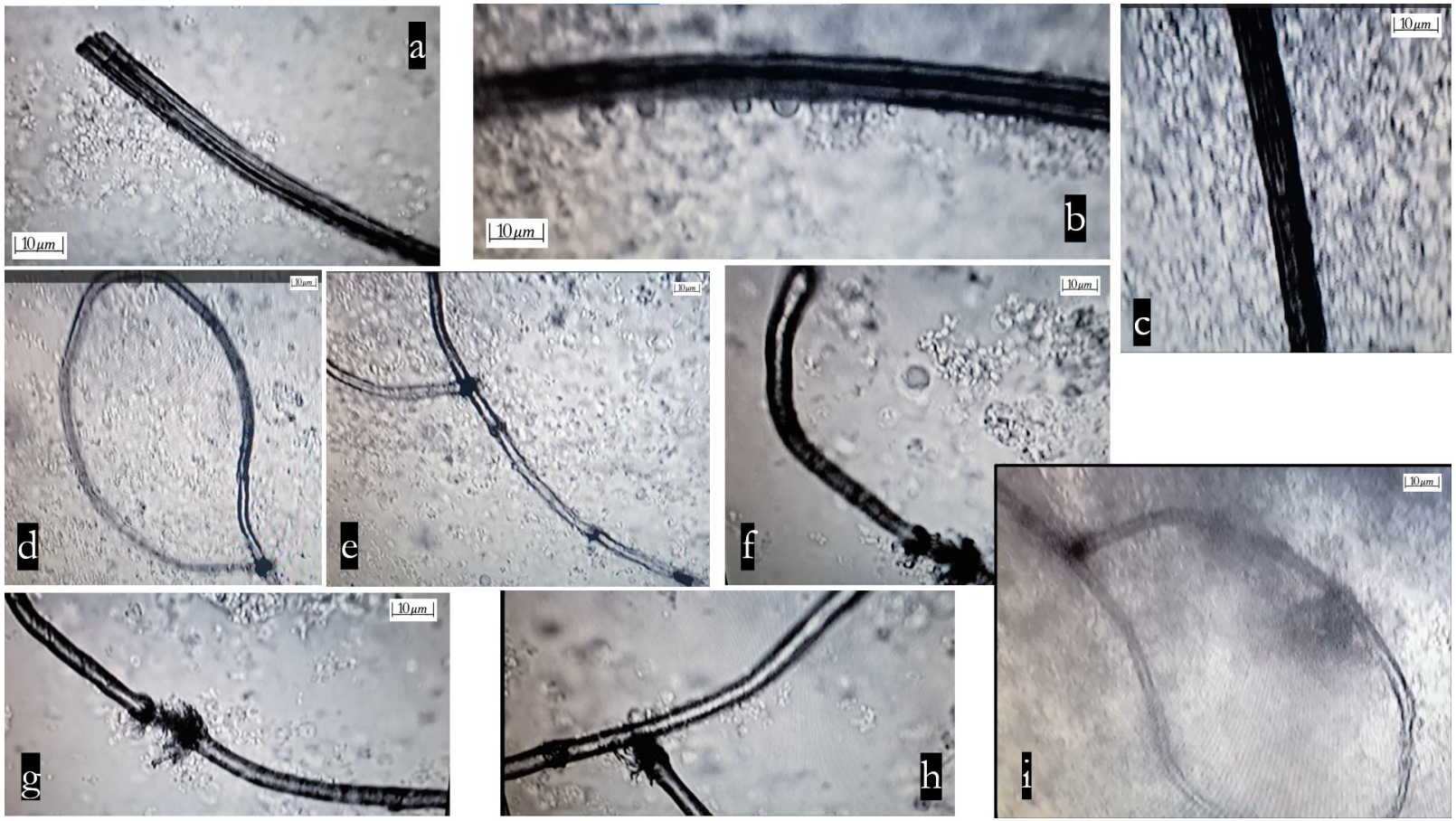

Figure 21. Findings of Moderna incubation study in plasma 2: (a) Day 133- dark pipe-like structure developed (100x); (b) with shedding bubbles (200x); (c) disappeared bubbles at Day 282(100x); (d) and (e) Day 133, snare-like lasso tubes (100x); (f), (g), and (h) Day 133, broken, disconnected points in the lasso-like tube (200x); (i.) Day 282, still the same figure maintained (100x).

Figure 22. Heat (Warming) Study of Pfizer - after 48 hours of warming at BT in normal saline: (a), (b), (c), (d), and (e): Floating well-assembled 3-dimensional geometric structures on the surface of the media after 48 hours of warming (36.5°C) on the heat template. Accelerated development was similarly matched to the findings in the 2nd~ 3rd week of the unexposed incubation study (400x).

4. Heat, EMF, and UV Exposures Study

1) Heat

Culture dishes were placed directly on a heat template set at 36.5 degrees Celsius overnight. The next morning assembled nanostructures were observed floating over the surface of the medium in more discernible and developed shapes than before the heat (warming) exposure. Two to three weeks were needed for the growth of structures at room temperature (15~20 ℃) whereas one evening was needed for the same growth at body temperature (Figure 22). The rapid development of nanostructures *in vivo* is probably significant to the impact of COVID-19 injectables in living human beings. It seems plausible that these kinds of assembled structures reacted to the direct heat emanating from the bottom of the dishes, dislodging from their place, and moving into the upper layer of the medium. When the newly thawed residual vials were incubated in the normal saline over the heat template for 48 hours, they showed more detailed and developed 3-dimensional structures floating in the media surface with no remnant material at the bottom — (accelerated developmental speed) overpassed 2~3 weeks upgraded as in the ordinary culture specimens.

2) EMF

a. Wireless recharger with a cellular phone

The culture dishes were placed on the cellular phone, set in the 5G streaming mode, over the wireless recharger for about 1~2 hours. Electric and magnetic measurements were taken through Triphase (see Figure 3-c). The field was measured as 300v/m, 0 in H-filed on the wireless recharger. The temperature was about 15~20°C. Reactions seemed to be the same in normal saline and in distilled water. Even after 1 hour of exposure to the wireless recharger with a cellular phone in operational mode, Moderna showed noticeable immediate changes. The floating materials abruptly became larger and more numerous with sharper and more rectangular edges (Figure 23).

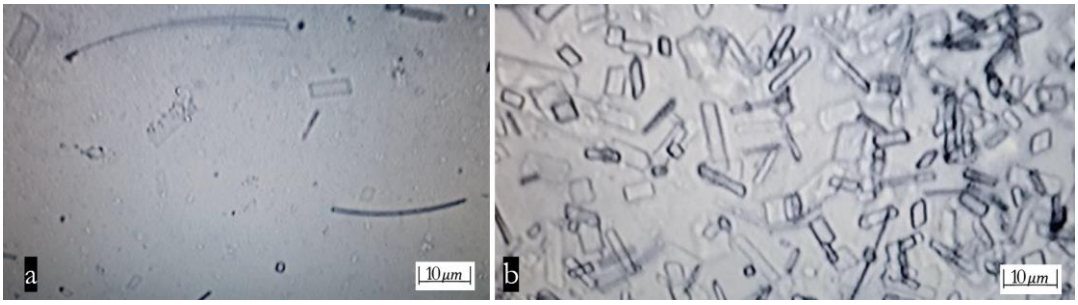

Figure 23. Study of wireless recharger for moderna in distilled water (Day 36, 200X): Moderna showed immediate multiplying and expansion response just after 1hour of exposure to the wireless recharger. (a) before exposure; (b) after 1 hour exposure.

In contrast, Pfizer showed no immediate response but, instead, after one month of exposure exhibited a delayed effect, a moderate proliferation of floating filaments (Figure 24).

In both Pfizer (Day 101) and Moderna (Day 36) culture dishes, after exposure to the wireless recharger, unidentifiable debris, likely micro-materials, seemed to disappear and leave in its wake a clean background.

B. External Hard Drive Exposure

EMF radiation on the surface of an external hard drive was measured at about 30v/m and 4μT in H-filed. The temperature was about 23~25°C.

After two hours of exposure to the external hard drive connected to a PC in operation mode, Moderna showed no noticeable effects, but Pfizer showed modest disruptive changes — slightly blurred boundary lines across structures with softer edges sitting at the bottom of the culture dishes. Basically, through the previous preliminary incubation study, at around 101 days incubation, the assembled structures in Pfizer in distilled water were progressively changed into a cloudy haze of more disrupted figures and finally disappeared, leaving only the floating filaments and ribbons attached to various bubbles. However, after 2 hours of exposure, the degradation appeared progressively more noticeable as most bubbles disappeared.

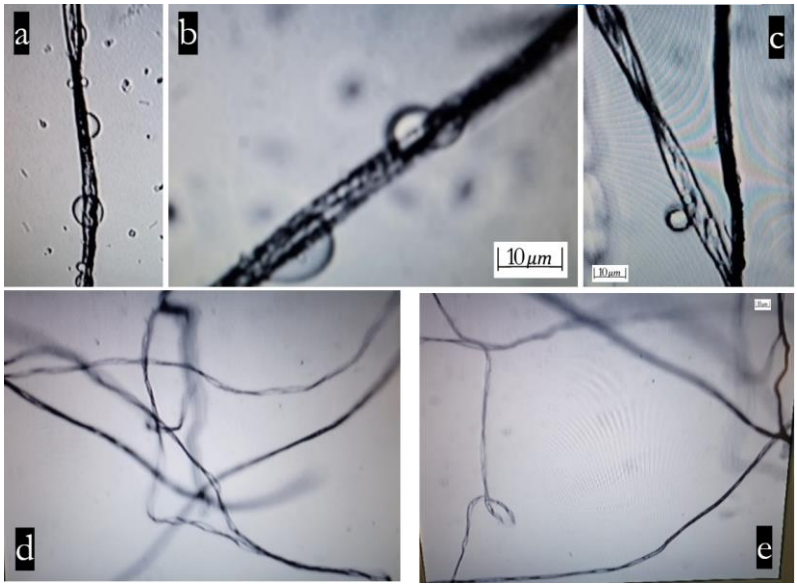

Figure 24. Wireless Recharger study for Pfizer: (a), (b), and (c) bubbly filaments before the exposure, Pfizer in distilled water, Day 95 (100x); (d) and (e) 1 month after the exposure, Pfizer in distilled water, Day 126 (40x) – disappeared bubbles and more multiplication.

Significantly, replacing the same Pfizer culture dish (Day 101) over the wireless recharger for only two hours of exposure returned the structures, partially, to their original sharper-edged and clearer forms (shown in the culture from Day 101). In other words, the diverse structures reassembled yet again in similar shapes to those before exposure to the external hard drive. See Figure 25 for details.

With the results of this preliminary study, it could be postulated that some kind of conditioned electric current can stimulate the nanostructure's activity, while some conditioned magnetic current can hamper their activity. According to our hypothesis, some detoxifying modalities could be effective in treating damaged organs from these complex forms of EMF exposure.

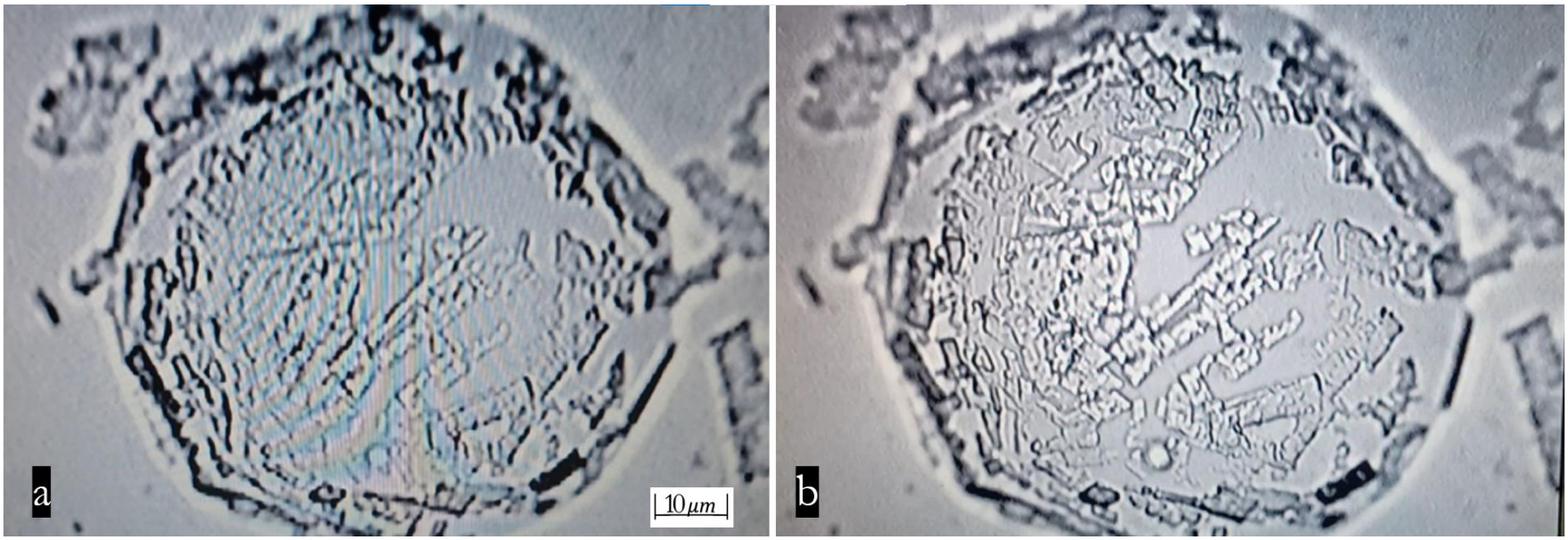

Figure 25. EMF (external hard drive/wireless recharger) study of Pfizer in distilled water (200X), 101 days of incubation: Pfizer study of exposure to external hard drive for 2 hours at Day 101 incubation in distilled water, and then followed by exposure to a wireless recharger for 2 hours. (a) after 2 hours of exposure to an external hard drive – more blunt edges and blurry alignment, more degraded than natural degeneration change; (b) after 2 hours of exposure to the wireless recharger immediately following exposure to the external hard drive- mild recovery (rescuing effect) appeared.

3)UV Study

There were no immediate differences observed in the short-term in the characteristics of both Moderna and Pfizer before and after exposure. However, through prolonged incubation, both samples did show more sustained self-assembled structures rather than ordinary developmental patterns as observed in other media absent UV exposure. This contrasts with the self-assembly observed at peak stage over six months to nine months in an ongoing observational study.

5. BIOCHEMICAL ANALYSIS OF THE VARIOUS "VACCINE" CULTURE MEDIA

A screening test for biochemical analysis of glucose, protein, pH, and occult blood via U-stick (Abbot, UroCor4, U040H012A 0) for the various injectable culture media was conducted to evaluate any changes to chemical components during long-term incubation. The U-stick, dipped in the culture media, revealed colorimetric changes which are summarized in Tables 12 and 13 (Appendix A). Of further interest are the unaided observable changes in the appearance of the culture media: Throughout the observational period, most translucent culture media appeared to morph from transparent to turbid, which was most prominent by day 150. This progression reversed back to its original state of translucence in the late stage of incubation (day 250).

Normal saline (NS) was used as a control for the study and showed all expected negative reactions in the glucose, protein, and 6.0 pH. During the first day, most media of diluted Pfizer (P1, P2, and P4) and Moderna with distilled water appeared as follows: a positive but weak reading in Glucose; a negative reading in Protein; 6.0 in pH; and a positive but weak reading in occult blood. The Pfizer booster (P4) showed two positives in the occult blood — perhaps as a false-positive from its interactions with peroxide. Noticeably, important results were negative in the protein on the 1st day of incubation of all studied specimens. Most of the culture media maintained an acidic state, pH 6 while glucose showed a weakly positive reading, except during the early incubation stage of Pfizer in distilled water (day 23). Of course, glucose should have been detectable since the FDA had reported that sucrose was a component of the "COVID-19 injectables," — especially Pfizer and Moderna.

Furthermore, according to the FDA's description, no protein should be present. Details are presented in the following pages in Figures 28 and 29. While proteins were not detected in the Moderna culture media throughout the entire incubation period, they were, however, present in the Pfizer media, a clear contradiction of the FDA's description. These included two positive (100mg/dl) readings in the early stage (day 23) which appeared progressively stronger as 300mg/dl incubated in the distilled water at day 79 stage, but finally became negative by the late incubation stage (day 288). The emergence of proteins appeared to be determined by diverging forms of culture media. In normal saline, a trace amount (10 mg/dl) was found during the late stage of incubation (day 266), but none were found in distilled water during the same period of incubation.

Some media revealed a positive reading (10 ~ 50 RBC/μl) on occult blood, but this reading could be interpreted as a false-positive because of potential exposure to hypochlorite or peroxidase. In the sodium bicarbonate (baking soda), however, Pfizer showed no signs of self-assembly at the bottom, perhaps having been disturbed by the Sodium Bicarbonate crystals. No floating materials, pH of 9 even after 1-month incubation appeared. Perhaps this is due not to the different pH effect, but to a disturbance caused by crystal formation at the bottom of the culture from exposure to baking soda

6. Recycling Pattern

When the dark seed-like particles, floating around the main body of skin extract (E1), were collected and incubated in normal saline, after 366 days, they showed a remnant or trace of the geometric self-assembled structures and a few pieces of the filaments similar to the findings from the original mRNA incubation studies. We can postulate that the recycling patterns appeared in between the incubation studies of the injectables and the formation of seed-like materials from the recipient's abnormal skin extracts (Figure 26).

Given the observed long-term behavior of the structures, we offer the following model that suggests the sort of recycling patterns that appear to be present in the pre-programmed nanoparticles themselves. The patterns appear to coincide with an interval period when the activity of self-assembly is dormant. When adequate ambient and internal conditions are met, we postulate that these conditions trigger the materials to activate and reconstitute nano-circuits/structures as outlined here.

Discussion

Since the WHO's declaration of a global pandemic on March 11, 2020, government-funded violations of civil and human rights — disguised as medical remediation of the pandemic — was actually leading to injurious and even lethal oppression in nations around the world. Since scientific pursuits necessarily presuppose open dialogue, critical thinking, and the rigorous testing of truth claims, we suspected, like many other researchers, that the program to address a global medical emergency was significantly more complicated than had been signaled. An additional motivation for this study, therefore, was the development of a comprehensive view of the WHO declaration that triggered the relentless push for total global compliance with "health" authorities.

Moderna Covid 19 Vaccine Ingredients (FDA)

- Messenger ribonucleic acid (mRNA), lipids (SM-102, polyethylene glycol [PEG] 2000 dimyristoyl glycerol [DMG], cholesterol, and 1,2-distearoyl-sn-glycero-3-phosphocholine [DSPC]), tromethamine,tromethamine hydrochloride, acetic acid, sodium acetate trihydrate, and sucrose.
- **The Moderna vaccine does not contain eggs, preservatives, or latex.**

Figure 29. Moderna ingredients.

Pfizer Covid 19 Vaccine Ingredients (FDA)

- mRNA, lipids ((4-hydroxybutyl)azanediyl)bis(hexane-6,1-diyl)bis(2-hexyldecanoate), 2[(polyethylene glycol)-2000]-N, N-ditetradecylacetamide, 1,2-Distearoyl-sn-glycero-3-phosphocholine, and cholesterol), potassium chloride, monobasic potassium phosphate, sodium chloride, dibasic sodium phosphate dihydrate, and sucrose.

***The Pfizer vaccine does not contain eggs, preservatives, or latex.**

Figure 28. Pfizer ingredients.

As with so many endeavors we undertake, certain periods of gestation, incubation or nurturing are needed to see emerge various forms of life, understanding, or purpose. Our purpose in this article has been to explain perplexing

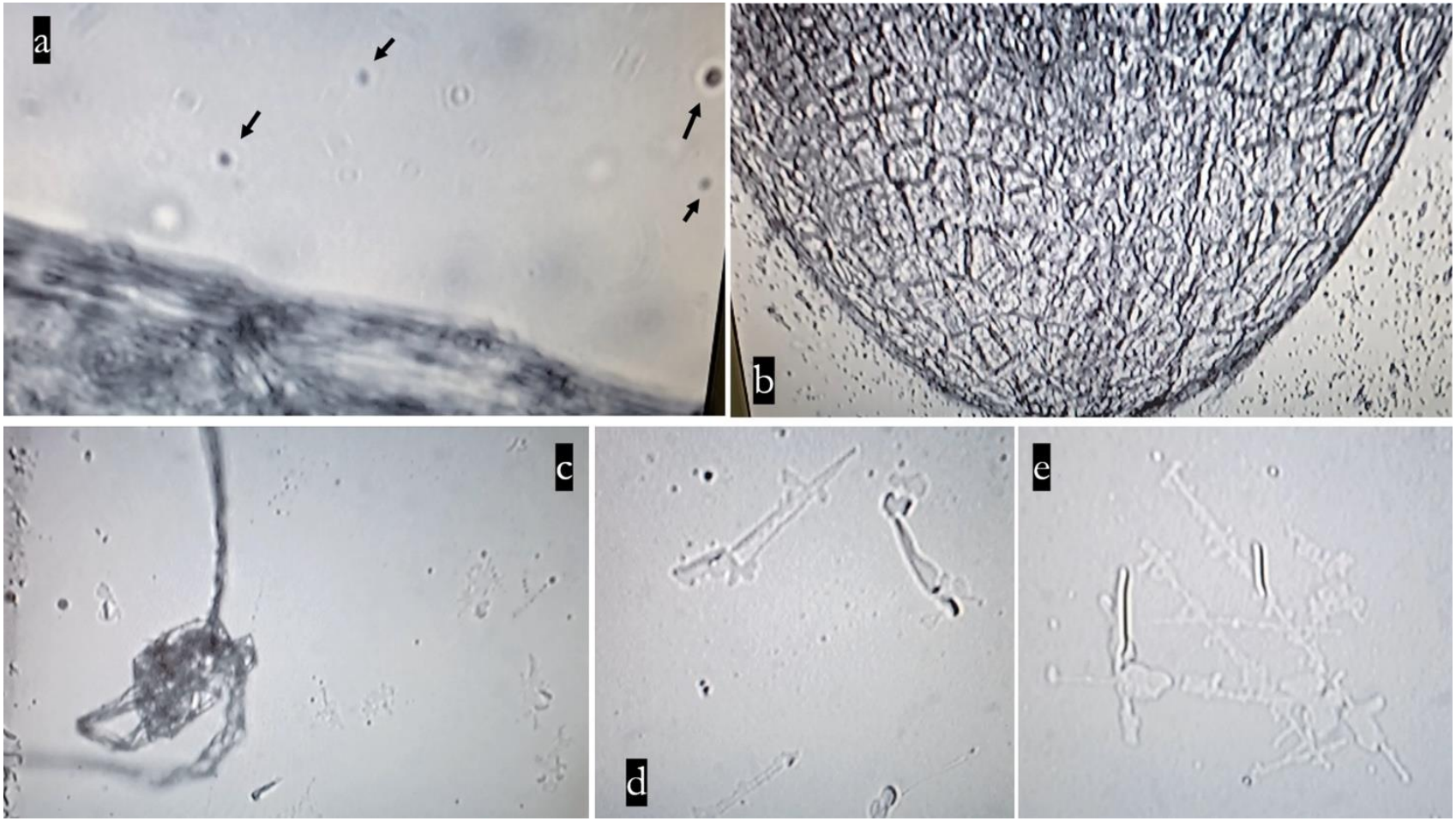

Figure 26. Recycling Pattern Study - Presumptive recycling pattern from the Moderna vaccinee's skin extract (E1) in normal saline: (a) seed-like tiny dark particles (arrows) floating around the skin extract 1(E1) in the normal saline media (400x); (b) tiny particles scattered around the vaccinee's skin extract, dark large material-crocodile skin-like structure (100x); (c) E1 seeds culture in normal saline - trace of the self-assembly at the bottom and floating filaments together after Day 366 incubation (100x); (d) and (e) Trace of the self-assembled geometric structures at Day 366 incubation (400x).

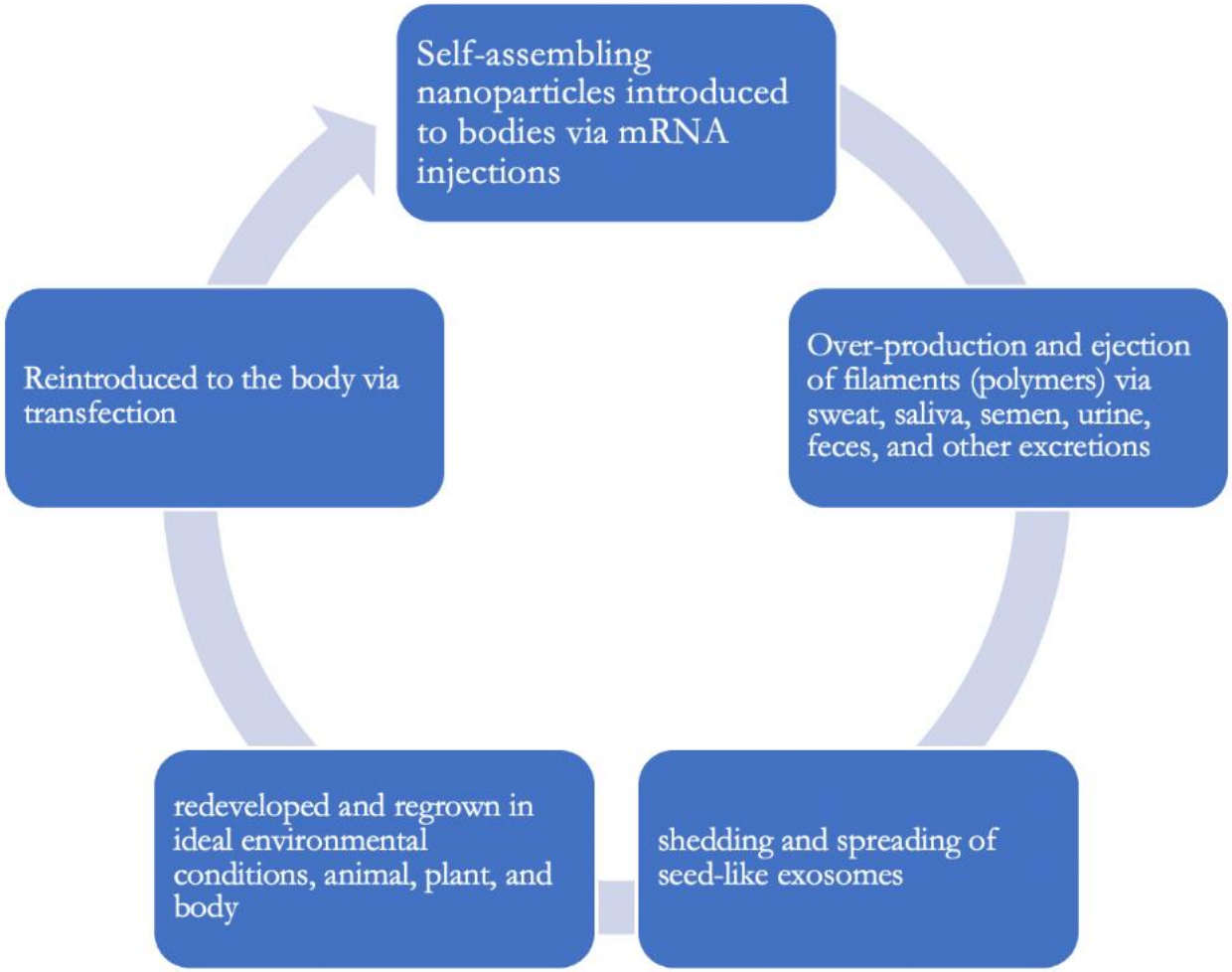

Figure 27: Proposed recycling pattern model.

phenomena appearing under the microscope and, thus, develop from incubation studies a greater understanding of the Covid-19 story. We begin discussion with reference to the FDA's public declaration of the injectable mRNA products marketed by Pfizer and Moderna containing ingredients reported in Figures 28 and 29. In this very journal, Segalla (2023a, 2023b, 2023c) has shown that many of the named ingredients, in Figures 28 and 29, are extremely toxic.

In summary, these products include the modified coding for the mRNA-inducing spike protein suspected of causing the harm inducing white clots discussed by Santiago and Oller (2023) along with others (e.g., Mead et al., 2024a, 2024b, 2024c); the lipid nanoparticle as a carrier (concerning the harm of which see the Segalla references); various adjuvants including the lipid nanoparticles themselves for immune stimulation; and built-in baffles consisting of the N1-methylpseudouridines substituted for uracil in the spike coding to slow down the degradation of the mRNA in the human body. Furthermore, AstraZeneca and Janssen report that spike-protein-encoded DNA encapsulated by Adenovirus is contained in these formulations. In contrast, Novavax is known to be a recombinant spike protein-based injectable. The bio-engineered spike proteins are harvested and assembled onto a synthetic lipid nanoparticle about 50 nanometers across, each displaying up to 14 spike proteins.

In our study of reactions to the foregoing four kinds of COVID-19 injectables by whole blood, plasma, and sperm, Novavax showed the most rapid cytotoxic effects. However, Pfizer and Moderna mRNA products showed more progressively injurious and ultimately lethal effects on living blood and sperm cells. They, furthermore, resulted in unprecedented self-assembling geometric chip-like structures, ribbons, filamentous structures, and encapsulated structures within structures.

Whereas we suppose that the announced ingredients and components of Figures 28 and 29 actually are present in the heavily marketed government-backed products, closer examinations and our own experimental studies show that there must also be unannounced nanomaterials that are invisible to standard microscopic examination. Also, despite reports offered for public review outlining ingredients, several additional studies would rule out the presence of ordinary DNA or RNA based on the absence of phosphorous and nitrogen which are abundant in those macromolecules (Hagimă, 2023a).

Experts in genomics recently discovered that the cancer-promoting SV40 gene is present in the COVID-19 Pfizer and Moderna injectables (Murakami, 2023; McKernan et al., 2023). The connection to cancer has been well established (Shah, 2006). If the spike protein is produced by the injected programmed mRNA, as hypothesized, the result could trigger a variety of toxic effects to multiple organs including vessels which could, finally, induce multiple organ failures — endothelial inflammation, immune imprinting, and the cytokine storm (Blaylock, 2021, 2022a, 2022b). The injection contents could damage the intracellular mitochondria and p53 genes, sabotage the body's ability to repair damaged DNA, induce immune system depletion, trigger frequent gene mutations and cancers, various autoimmune diseases, as well as reproductive failures (Alavi & Kheradvar, 2012; Xie et al., 2021; Idrees & Kumar, 2021; Classen, 2021; Seneff et al., 2022; Gat et al., 2022; Mead et al., 2024a, 2024b, 2024c).

Through biochemical analysis of the injectable culture media, the most significant finding was the presence of protein. If the media are alkaline, or if they contain chlorhexidine (0.25%), the media could reveal a false-positive. However, most culture media were maintained as acidic throughout the entire incubation period, which left no possibility for chlorhexidine to be introduced to the

experiment. If there were no exposures to chlorhexidine as our study has ensured, how and from where could protein have emerged?

During the initial incubation period, the presence of protein was not detected. Without any bacterial contamination, protein could only be produced by the injectable itself in the distilled water or normal saline media. According to Cell-Free Protein Synthesis, described by Endo (2021), the bubbles observed in our study could be the result of self-synthesized proteins, which could be toxic. Most interesting was the initially undetected, then detectable (day 23~day 82), and ultimately once again undetectable progression of protein synthesis. We discovered what, initially, appeared to be a coincidental relationship between (a) the developmental patterns of self-assembled nanostructures (peak stage of development, 2 to 6 months), (b) the behavior of hydrogel (initially transparent for 2 to 3 weeks, later gel-like emulsion in nature until day 150, and finally returning to its transparent consistency) and (c) protein production to some degree. Further studies are needed to clarify the central issues regarding all three of these apparent dynamic relationships. Turning to Burkhardt's analysis (2022), we remind readers of the effects of the spike protein and the synthesis of many kinds of proteinaceous materials discovered in blood clots (approximately 323 kinds of proteins) — especially 4 kinds from endothelial tissue damage.

Given the analyses we offer here, we speculate that the materials in the injectable products produce not only the publicly reported spike-protein induced presumably by the modified mRNA, but also there appear to be various abnormal toxic protein secretions, likely from either the presence of the nanostructures themselves or from cross-domain bacteria via hybrid synthetic biology (Maervoet et al., 2017). Further analysis is welcomed.

In reporting that mistranslations of modified mRNA could produce abnormal protein synthesis and stimulate the human immune system to recognizing the abnormalities as foreign proteins, Paul Marik and his colleagues (Front line COVID-19 Critical Care Alliance, 2023) proved the risk of ribosomal frameshifting caused by replacing uridine with N1-methylpseudouridine to avoid its natural destruction and to ensure long-lasting antigen development, because of spike protein synthesis (Mulroney et al., 2024). Some researchers have reported that COVID-19 injectables may be causally related to pathophysiology of amyloidosis and prion disease (Perez et al., 2022; Classen, 2023; Leung et al., 2023).

According to Dhuli et al. (2023), using mass spectrometry methods to analyze serum in the blood of "long COVID" patients, both viral spike protein and injectable spike protein were found together during analysis. This discovery means that "long COVID" could be correlated with both the long-lasting viral spike as well as injectable-induced spike protein.

Significantly, the two spikes differed markedly. Their work appears to confirm that ribosomal frame shifting occurs post-jab, which only deepens earlier speculation that abnormal protein production may also be occurring. If these observations are valid, the abnormal protein synthesis earlier discussed could trigger a range of unprecedented varieties of disease of the sort being described, for instance by Mead et al., (2024b, 2024c).

Through our observational studies of blood and semen samples (composed largely of living cells), the COVID-19 injectables showed definite and consistent cytotoxicity but in varying degrees. Novavax and AstraZeneca, especially, showed even more rapid toxic effects than did Pfizer and Moderna, even though the former are not mRNA products. This variability could prove meaningful to the mounting evidence of the cytotoxicity of the spike protein itself.

Beyond the above-mentioned sequalae of infections or injections, many kinds of medical evidence were reported about the toxic spike protein characteristics — loss of elastic fiber could induce rapid skin aging and vascular rupture. Moreover, postmortem reports written by both medical professionals and embalmers have noted significant increased signs of bizarre thrombosis — likely due to the presence of unique, never-before-observed extremely elongated fibrous clots, categorically distinct from ordinary common blood clots, extracted from essentially every conduit system carrying fluids in the body.

As we reported here, we have isolated numerous and various unidentified materials — a few μm in size — beyond the nanoparticles described in FDA reports for the mRNA injectables, in the Pfizer and even more so in the Moderna products.

Having concluded various experiments and careful observational studies, we infer that the materials and their observed stages of development are not natural. They are synthetic, and elemental seeming to govern a well-programmed process of structural self-assembly. That their provisional final production could be described as artificial has already been suggested in the numerous articles referenced so far.

The results of experiments with exposure to heat and electromagnetic energy were significant: short-term exposures showed remarkable changes in the self-assembled structures. Ultraviolet radiation, visible light, temperature, nitrogen, sources of carbon in the air, electromagnetic fields, various wave frequencies, and other factors can evidently trigger nanoparticles to react — whether to assemble or disassemble what appear to be pre-programmed structures.

Suberi et al. (2023) report on recent developments with a new mRNA delivery vehicle that utilizes optimized biocompatible poly(amine-*co*-ester) polyplexes. They note that the new system is a highly customizable polymer for inhalable vaccine delivery to the lung. If these previous injectables as programmed nanoparticles, which later produce polymers, are introduced into the deltoids of recipients — as they were through experimental random samples — the next generation of "vaccines" could be delivered through nasal inhalation or skin patches using similar polymer-based materials via programmed nanoparticles.

Sasha Latypova, an executive and researcher for the pharmaceutical industry, discovered an extreme deviation in side effects among the batch-to-batch vials of mRNA COVID-19 injectables. In a normal world, this sort of wildly uneven deviation would be intolerable in ordinary pharmaceutical products receiving routine oversight by regulatory bodies adhering strictly to established protocols and safety guidelines. Nevertheless, as the public has been reminded continually, we are living in a "new normal". How, therefore, might we understand more generally this obvious deviation from the old normal? One way is to consider intentionality. These products were meant to serve foremost as experimental injections for the whole of humanity — including all ethnicities, sexes, and age groups.

This depiction squares with the FDA approval letter of the Comirnaty (Pfizer product; FDA, 2021), the post-marketing requirement, in infants under 6 months of age, the study completion of July 31, 2024, and the final report which is to be submitted by October 31, 2024. Worth nothing is that in the accompanying documents for the injectable products all details referring to the factories where they were manufactured were conspicuously redacted, which begs larger questions about secrecy undermining informed consent.

As regards "vaccine" exposure to electromagnetic energy, preliminary observations show that the materials in the injectables react positively to wireless cell phone rechargers while they react negatively to external hard drives. As electromagnetic frequency-sensitive materials, it is plausible that the injectable contents are designed to act as a kind of semi-conductor. Many researchers have called attention to the biohazardous effects of electromagnetic energy fields to the human body, especially causing carcinogenesis, neurodegeneration, damage to reproductive cells, and rapid-developing fetal cell damage (Ilori et al., 2019; Kashini et al., 2023; Noor-A-Rahim et al., 2022; Dasdag et al., 2015; Russell, 2018; Moon, 2020).

Wireless rechargers or external hard drives are useful and very common personal electronic devices. If recipients of the experimental injectables ("vaccines") have these materials circulating in their body and if they use these personal electronic devices, the devices themselves may, beyond routine electromagnetic field exposure, increase harm to their health, particularly to cellular regeneration, as the contents react synergistically with ambient radiation.

If the injectable contents are designed, in part, to serve as both software and hardware for the clandestine construction of intracorporeal networks as Kyrie and Broudy (2022) suggest, the contents likely interact with electromagnetic energy fields outside the body. In the present developmental stage of mobile communications networks globally, we urge researchers to reproduce our efforts or setup alternative studies to better understand what remote effects there may be on human/animal/plant biology in the face of forthcoming 6G and 7G iterations of WiFi and LiFi. Despite rampant speculation in the literature regarding the use of COVID-19 injectable products and the development of wireless body area networks, abbreviated to WBAN (Jornet & Akyildiz, 2013; Jing et al., 2023), more interdisciplinary work is needed. Such studies would aid in the development of possible electromagnetic treatment modalities for recipients seeking alternatives to either standard chelation protocols or escaping entirely from an electromagnetic energy-polluted environment.

Incubation studies, furthermore, showed that distilled water served as an ideal medium to reveal unique changes in the growth of injectable contents. Since distilled water is unadulterated and undisturbed by its own electrochemical properties, we postulate that it has latent potential to manifest the specifically engineered developmental pathways, the intended characteristics of the injectable contents, and to respond, as programmed, in easily observed ways to electromagnetic energy.

In the plasma reaction, we speculate that the self-assembly process of nanomaterials was hampered by the profusion of blood cells at the bottom of the dish where space for self-assembly was already occupied. However, very few small chips were found at the bottom of the plasma dish by one month incubation and then disappeared. Later, filaments and pipe-like structures, even relatively small and few, appeared and maintained their morphology until the late stage of incubation. This finding indicates that initial assembly at the bottom is not a prerequisite to the later development of the filamentous structures. So, *in vivo*, it could be possible to produce various nanofilaments or carbon nanotubes without any prerequisites whatsoever.

In analysis of blood clots from vaccinated persons, a few filament-like structures were found attached to brownish homogeneous cloudy white clots extracted from the middle layer of whole blood sediment. When in close proximity to an electromagnetic field, the filaments could possibly trigger the formation of a clot and, thus, disturb free blood or lymph flow. Given their microscopic

size and wide distribution throughout the body, if these foreign materials interact with either inside or outside sources of energy, as the literature states, they could well become elongated, enlarged, and serve as mysterious modes of morbidity and eventual mortality.

Beyond the pathophysiology described above, the theoretical work of nanotechnology described in the decades of literature appears to be present in the practical application of the mRNA "vaccines", especially in Pfizer and Moderna. Anecdotal observations of patients suffering from a range of sudden extraordinary injuries in the wake of the initial rollout of the "vaccines" triggered our inquires both in the laboratory incubation studies and in the published literature across biology, nanotechnology, electromagnetic field science, and materials engineering. Taken from the original "vaccine" contents, the incubation studies were fruitful in helping to identify various foreign materials and to better understand their possible pathophysiology *in vivo*. Other researchers, however, have offered alternate opinions that the materials could simply be sodium chloride (NaCl), and other contaminants, and their observed behaviors simply the result of natural crystallization. That whole class of objections can be addressed with an appeal to physics.

Fractals have long been known to form in linear dimensions through regular predictable patterns, and when environmental factors are optimal, such as oscillation in the material universe, fractals develop higher structural dimensions (Dubuc et al., 1989). Moreover, it has been widely observed that the residue of most evaporated solutions features similar crystals — especially NaCl and various kinds of electrolytes and even in water itself via the hydro-glyph mechanism (Wakeling cited in Bailey, 2022). It was, therefore, necessary that the injectables be cultured in media that maintained an uninterrupted liquid state which would serve to verify that these sorts of self-assembled structures are not the same natural crystals induced by normal evaporation processes.

Significantly, mRNA technology is often marketed in terms of software as a kind of operating system or technology platform (per Moderna's Website). Although Moderna's original characterization of mRNA technology as a computer program has been deleted from their website, we offer it to readers as a reminder of their prototypical concept:

> Recognizing the broad potential of mRNA science, we set out to create an mRNA technology platform that functions very much like an operating system on a computer. It is designed so that it can plug and play interchangeably with different programs. In our case, the "program" or "app" is our mRNA drug — the unique mRNA sequence that codes for a protein (Moderna quoted in many articles, e.g., see Reuters, 2021; Martin, 2024).

The geometric patterns of most of the self-assembled structures, as in electronic circuits or 3-dimensional chip-like structures, progressively degraded after about day 80 during incubation of the Pfizer booster (injection number 4, P4), which has a different timeline from the other injectables (P1, P2 & Moderna), while similar degradation patterns were also manifested. This means that the injected nanomaterials appear to be programmed to behave in the manner observed and to carry out regular intervals of self-assembly and disassembly. The entire process, we theorize, must be periodically re-enforced, likely through the prescribed regimen of new "booster shots" per CDC recommendations.

Occasionally, other researchers have reported microscopic findings of filamentous structures in commercially branded normal saline. Despite apparent similarities in morphology with injectable filaments, the structures found in saline are slightly different in their behavior and growth patterns. Noteworthy were the various unusual structures that appeared: unique striated curled ribbons and

various filaments, scaled like snakeskin, that seemed to contain hollow compartments as in bamboo shedding bubbles. These structures proliferated throughout the medium and were elongated, twisted, knotted, discolored, and varied in texture.

During our observational studies, the filaments that appeared to shed bubbles were consistently active. We urge that further studies are needed to differentiate whether these filaments derive from the basic media or from the injectable product itself. Regardless, isolating their origin could represent a significant discovery for the question of whether many, or even, most other pharmaceutical products and/or manufacturing processes are already contaminated by nanotechnology. It is sobering to think that the covert technology may not be limited to the COVID-19 injectables. Highly detailed geometric self-assembled structures featuring right angles were observed at the bottom of the culture dishes (in a well-maintained liquid state) while dislodged floating structures in the upper layer appeared during the 1st few weeks as noted.

Research in nanomaterials engineering shows that Biohybrid Magnetic Robots (Microalgae-based Magnobots) could be produced and propelled throughout the body by a variety of triggering factors: electromagnetic energy, change in pH range, manipulation of glucose levels, and by varying light spectra with the aim of targeting certain tissues (Li et al., 2023). Observations during our incubation studies suggest the presence of magnobots, especially in the Pfizer sample.

Our culture studies revealed that the Pfizer products in simple distilled water produced a variety of transparent ribbons, thin film-like membranes, coils, and spirals even without exposure to special supplements or ambient energy sources. These patterns of growth and appearance in the culture media could not be explained apart from mechanisms of action peculiar to nanotechnology (Cao, 2019; Truong et al., 2016). During the initial stage of incubation with various electrolyte solutions, the self-assembly process was possibly interrupted to some degree by the crystallization taking place in the various media and solutions and their concurrent spread across the bottom of the dish.

Various kinds of transparent ribbons, films, coils, and spirals appeared in the Pfizer sample incubated in distilled water. These were very similar in structure to the micro- and magnetic-nanorobots already presented in numerous scholarly papers (Zhou et al., 2021). These structures, according to numerous researchers, could serve as signal conductors, biosensors, switches, and/or electronics devices needed for the transhumanist movement toward a post-human society (Kyrie & Broudy, 2022; Mousavi et al., 2021; Bailey, 2022; King Abdullah University, 2021; Alamoudi et al., 2021; Marsudi et al., 2021; Zhang et al., 2019; El-Husseiny et al., 2022; Shiu et al., 2022; Zhou et al, 2021; Johnson, Broudy & Hughes, 2024a, 2024b, 2024c, 2024d). These structures could also serve as nanodevices such as plasmonic antennae or as transceivers for terahertz band communications (Jornet & Akyildiz, 2014). Nanostructures are known to be stimulated to grow and carry out functions from various triggers: visible light, temperature (heat), electromagnetic fields, ultraviolet radiation, water, carbon and oxygen via air, special electrolyte-Ca^{++}. These phenomena we have been able to confirm through longitudinal observations.

Noteworthy, also, is observed phenomena in the uppermost layer and the middle layer of the culture media likely due to the mass and weight of the structures. During the late stage of incubation of Pfizer in distilled water at about day 337, transparent bundles of wire-like hollow tubes emerged and, in the uppermost layer, appeared similar in structure to skin extract 2 (another anonymized patient designated simply as E2). These filaments were different in character, however, from

ordinary filaments. As of this writing, the tubes have since developed into unique striated curled ribbons.

This process of dynamic and changing morphology represents a key signifier of another kind of recycling pattern likely related to injection and the production of skin extracts observable from long-term incubation studies. Furthermore, the bundles and ribbons could be more durable and long-lasting silica, or they may be synthetic graphene-coated polymer nanotubes, or similar nanowires serving as conductors or semiconductors survivable to temperatures from 1000°C to 4,000°C according to the relevant research literature (Hagimă, 2023b). While the presence of foreign materials in the human body triggers various natural detoxifying processes, some materials nevertheless persist despite all attempts to chelate or dismantle them. Aluminium, for example, has long been known to lodge in the brain for long periods and the outcomes are often neurological disorders and disease (Shaw, 2017). We infer from our observations, therefore, that critical discussion of possible treatments or regimes of detoxification are necessary.

Especially with regards to test subjects who have been jabbed within one to two weeks, silica water may be helpful because it could potentially disturb the early stage of assembly of the chip-like structures. In the later stage, say, three weeks after injection, colloidal gold or silver (3-5 nm in diameter and 10-20 ppm) has been observed to attach to, disrupt, actively degrade, and ultimately dissolve various nanostructures. The longer-term results of such treatment protocols are being examined in ongoing experiments. Mica also has been shown to exhibit similar positive effects.

Routine exposure to heat saunas may also trigger nanomaterials to dislodge from tissues and escape through sweat gland pores. We postulate that recovery of damaged organs and normal blood flow can return with the use of gold or silver, or other specialized crystals with their own unique healing frequencies. Since electromagnetic energy stimulates the formation of the observed nanostructures, regular (re)grounding (earthing) the body can help discharge over-accumulated electromagnetic energy in tissues. Avoiding unnecessary excess exposure to electromagnetic energy can also be beneficial. Personal electronics, such as smart watches, smartphones, wireless earphones, Wi-Fi routers, and all other forms of electromagnetic energy pollution, should be significantly reduced if not eliminated. The various remedies we describe here could be applicable as regimes for "vaccine" detoxification while subjects bear in mind the unique personal variance of each response.

Conclusion

A review of government white papers and scholarly literature in biotechnology, nanotechnology, materials science, and electronics engineering combined with longitudinal incubation studies reveal compelling evidence of various fundamental corruptions. Injectable modified mRNA platforms — widely known as "vaccines" — inject in the deltoids of billions of human beings are evidently adulterating what is already there.

Observational studies and comparative analysis suggest that intentional contaminations appear in the "vaccine" vials, in blood samples extracted from test subjects exposed to the "vaccines," and in the subsequent shedding of synthetic biologicals (Woodruff & Maerkl, 2016). Both the morphology and behavioral characteristics of these observed phenomena suggest that far from being pure (Finn, 2011 p. 138), these injectables are composed of, hitherto, undisclosed additional engineered components responsive to a range of internal and ambient forms of energy, all of which are traceable to and described throughout the scholarly literature.

Profound deviations from the generally understood meaning of the "vaccine" marketing slogan and its claim of "safe and effective" appear in observations of the "biologicals" under the microscope. Excess deaths, incidences of "turbo" cancer and various autoimmune diseases reported globally since the rollout of the "injectables" show a suspiciously high correlation. The perversions we have described suggest a clear correspondence to the communications infrastructure now appearing under construction in the long-planned well-funded Internet of Bodies, the IoB (Celik et al., 2022), a kind of synthetic global central nervous system — the details of which are also widely discussed and illustrated in the scholarly corpus. Biohybrid Magnetic Robots, in particular, represent a significant concern for researchers attempting to make sense of the responsiveness of these "biologicals" to energy sources. We echo the calls of other researchers engaged in similar studies: until the components can be verified and their long-term effects understood, a necessity flouted by calls for Emergency Use Authorization, an immediate global ban is needed.

Responsibilities of the Authors

Youngmi Lee: conceptualization, research design, imagery analysis, data curation, writing original draft.

Daniel Broudy: Imagery analysis, data curation, editing, drafting, revising.

Legal Disclaimer

Appendix A

In this Appendix tables referred to above beginning on page 1196 in the text are presented.

Table 5
Comparison between Semen and Blood Media with Varying Degrees of Incubation with Injectables

	Pfizer 1		Pfizer 2		Pfizer 4		Moderna		AZ	
Plasma 1 from a non-vaccinee	D24	D146					D24	D146		
	C +/-	C -					C +/-	C -		
	F -	F -					F -	F+/-		
Plasma 2 from a non-vaccinee		D146						D146		
		C -						C -		
		F +						F +		
Semen 3 From a person who received 2nd jab of Pfizer	D37	D362	D37	D362	D37	D362	D37	D362	D37	D362
	C +	C +(1-2Ds)	C +	C -	C +	C -	C ++ (2 Ds)	C + (1-2Ds)	C -	C -
	F+(Rope)	F +	Nano worm+	F ++	F +	F +	F +	F +	F +	F ++++
			F +	SH +		f/b	T +	R +		SH +/-
			R +							

D = day of observation after incubation; Ds = dimensions; C = geometric chip-like assembly; F = filaments observed; R = ribbon-like material; T = object appearing like a piece of tape; SH = intact sperm head; f/b = contamination attributed to fungus or bacteria

Table 6
Cytotoxicity Observed in % of Motility of Sperm Cells Over Time with Various Chemicals Using the Healthiest Semen Sample (Semen 4) Available for study

Time lapse	Korean Spirit (proof 20)	Red wine	Beer	Mica	Colloidal Gold (GNP1)	Silica water	Vitamin C	Calcium hypochlorite $Ca(OCl)_2$		Incubation media† of E1
								0.001%(1X)	0.01%(10X)	
0	0								0	
30 m	0	1%							0	
1.5 h	0	1%	0	10%	0	0	0	0.1%	0	10%
3 h	0	0	0	0.1%					0	

E1 = Skin extracts from Moderna vaccinee; † = long-term incubation media of E1 with normal saline; m = minute; h = hour

Table 7
Growth Differences between the Media with mRNA Vaccines (Pfizer & Moderna)

	D/W				**N/S**			**H/S**				**$Ca(OCl)_2$ (1X) 0.001% †**			**ClO_2(1/100 X) 1ppm †**		
Day	D 41	D60	85	D297	D51	D95	D306	D42	D60	D85	D297	D42	D85	D311	D18	D111	D 230
P1	C+++ F + R ++	C++ + F + R++	C + F++ R++ S+++	C - F +++ R+ S +/- W +	C++ (3Ds) F + R ++	C+++ F ++ R +	C +/--- F +++	C++/- F -	C - F -	C+/- F +	C - F +	C+++ F -	C++ (3Ds) F +	C - F +	C+/---- F -	C ++ F -	C - F +
P2			C - F +	C - F ++	C + (1-2Ds) F -	C++ (2Ds) F+ (twisted)	C - F + (twisted, bubbly surfaced)	C++/- F +	C - F -	C - F++	C- F +	C+ F -	C +/- F +	C +/- F +++			
P4					C +++ (3Ds) F +	C +++ (1- 2Ds) F +	C - F +++ (shorter)	C + F -	C+/- F -	C+/- (1-2Ds) F +	C+/- (1-2Ds) F +	C + F -	C+++ (3Ds) F ++	C - F +++			
M	C ++++ F + (branched end)		C +++ F + R +/-	C - F +/- R -	C +++ F + R +	C++ F +/-	C - F - Circle+ at the bottom	C +/-- F -	C+/- (1-2Ds)	C+/-- F +	C - F +	C + R +++	C++ F+++ R++	C - F ++ (shorter)	C+/---- F -	C +++ F -	C - F +

C = chip like assembly at the bottom; F = Filaments in the middle layer; R = Ribbon floating in the upper layer; S = Spirals; W = transparent wires; Ds = dimension; D = incubation days; † = applicable standard concentration for drinkable water

Table 8
Calcium Hypochlorite, $Ca(OCl)_2$ Dose-dependent Study for Covid-19 Vaccines

`	Pfizer(P1) for adult				Pfizer(P2) for Children				Moderna				AZ	NV
Days	D85		D311		D85		D311		D85		D311		D85	D85
	C	F	C	F	C	F	C	F	C	F	C	F	C/F	C/F
D/W	+++	++ Ribbon	-	+++ Wire	-	+	-	++	+++	+	-	+/-	-/-	-/-
1X † (0.001%)	++ (3Ds)	+	-	+	+/-	+	-	+++	++	+++	-	++, shorter	-/-	-/-
10X ‡	+	++	+/- (1-2Ds)	+++	+/-	++	-	++	-	+++	-	++++, bubbly	C - F+	-
20X	+	+/-	-	+/-	+/-	+	-	-	-	++, small	++	++ bubbly	-/-	C - F +
30X	-	-	-	+/-	-	-	-	+/-	++	+/-	+/-	++	-/-	-/-
50X	-	-	-	-	-	-	-	-	-	-	-	-	-/-	-/-

X = grade of concentration; C = chip-like assembly at the bottom; F = Filaments in the middle layer; Ds = dimension; D = incubation days; D/W = incubation in distilled water for the comparison; AZ = AstraZeneca; NV = Novavax; † = applicable standard concentration for drinkable water; ‡ = standard concentration for swimming pool disinfection

Table 9
Chlorine Dioxide, ClO_2 Dose-dependent Study with Covid-19 mRNA Vaccines Incubation

	Pfizer							Moderna						
Days	D18	D85		D111		D230		D18	D85		D111		D230	
C/F	C	C	F	C	F	C	F	C	C	F	C	F	C	F
1/400 X	+/--	+++	-	+++	-	+/--	++	+/-	-	-	++++	-	+/---	+
1/200 X	+/--	+++	+	+++	-	-	+	+/-	-	-	++++	-	+/----	+
1/100 X †	-	++	-	++	-	-	+	f++>b	-	-	+++	-	-	+
1/64 X	-	-	-	+	-	-	+	-	+/-	+	+	-	-	+
1/32 X	+/--	-	-	+/-	-	-	+	+/--	-	-	+	-	-	+
1/16 X	+/--	-	-	+/-	-	-	+	+/-	-	-	+	-	-	-
1/8 X	+/--	-	-	-	-	-	+	-	-	-	-	-	-	-
1/4 X	+/-	-	-	-	-	-	-	+/--	-	-	-	-	-	-
1/2 X	+/--	-	-	-	-	-	+	-	-	-	-	-	-	+
1X ‡ (100 ppm)	+/----	-	-	-	-	-	+	+/----	-	-	-	-	-	+

X = diluted concentration; C = self-assembled geometric chips-like structures; F = filaments; f>b = more fungal contamination than bacterial contamination; D = incubation days; † = applicable standard concentration for drinkable water; ‡ = concentration for disinfection (aseptic process for surgical instruments)

Table 10
Hydrogen Peroxide, H_2O_2 Dose-Dependent study with the mRNA Covid-19 Vaccines Incubation

	Pfizer				Moderna			
Culture D	D5	D105	D203		D5	D105	D203 (D217)	
Chips Filaments	C F	C F	C	F	C F	C F	C	F
1/500X	C++	C+/-	C +/---- (1~2Ds)	-	C +++	C+++(3Ds)	C -	+++longer
1/200X	C++	C+(1~ 2Ds)	-	-	C+++	C+++(3Ds)	C ++++ (2~3Ds)	-
1/100X (0.03%)	C++	C++(2Ds)	C +/---- (1Ds only) disruption	-	C+++	C+++(3Ds) F + S +	C + (2~3Ds)	++ shorter

X = diluted concentration; C = geometric chip-like assembly; Ds = dimension; F = filaments; S = spirals; D = incubation days

Table 11
mRNA Vaccine Incubation Study with Various Mineral or Supplementary Solutions

Vax	Pfizer									Moderna								
Days	D9			D36			D253			D9			D36			D253		
C/F/O	C	F	O	C	F	O	C	F	O	C	F	O	C	F	O	C	F	O
N/S	+++	-	NP	++++	-	-	+/-	+++	-	++	-	NP	+++	-	-	-	+	-
Si Water	+/-	-	-	+/-	+/-	NW	+	++	-	++	-	-	+	+	-	-	+	-
GNP2	+	-	-	+	-	-	++	++	f++	++	-	-	++	-	-	++	++	-
GNP3	+	-	-				-	+	-	+	-	-				-	++	-
GNP4	++	-	-				-	+	-	+	-	-				-	++	-
SNP	++	-	-	++	-	-	-	+/-	f+++	+++	+	-	+++	++	-	-	+	b++
EDTA	+	-	-	++	-	-	-	+/-	f++	++	-	-	++	-	-	-	+++	-
MICA	-	-	-	+/----			-	+/-	f+++	+/-	-	-	+/---	-	-	-	+/-	f++
Myrrh	?	?	bub	?	?	bub	?	?	Solid									

C = geometric chips; F = filaments; O = others; b = bacterial contamination; f = fungal contamination; bub = bubbly; NP = nanoparticles; NW = nano-worm at the bottom; Solid = solidification

Table 12
Biochemical Analysis of Various Vaccine media along the culture period (via U-stick)

	Vaccine + media	Vaccine type	Culture Period	Condition	Glucose +/- ~ ++++ 100~2000mg/dl	Protein +/-~++++ 10~1000mg/dl	pH 5.0~9.0	OB +~+++ 10/5-/250 (RBC/μl)
1	P1NS	Pfizer 1	D266	EMF/5G	+(250mg/dl)	-	6.0	-
2	P4NS	Pfizer 4	D266	EMF/5G	+/-(100mg/dl)	-	6.0	-
3	P1DW	Pfizer 1	D266	EMF/5G	+(250mg/dl)	+/-(10mg/dl)	6.0	+(10RBC/μl)
4	P1DW	Pfizer 1	D23	Overnight UV	-	++(100mg/dl)	6.0	+(10RBC/μl)
5	M1DW	Moderna 1	D224	-	+/-(100mg/dl)	-	6.0	-
6	M1DW	Moderna 1	D23	Overnight UV	+/-(100mg/dl)	-	6.0	-
7	M2DW	Moderna 2	D221	EMF/5G	+++(1000mg/dl)	-	6.0	++(50RBC/μl)
8	P1BS	Pfizer 1 (D27)	D1 (D27)	Overnight UV	-	+++(300mg/dl)	9.0	+(10RBC/μl)
9	P1DW	Pfizer 1	D49	Overnight UV	-	++(100mg/dl)	6.0	+(10RBC/μl)
10	P1DW	Pfizer 1	D82	Overnight UV	-	-	6.0	+(10RBC/μl)
11	M1DW	Moderna 1	D45	Overnight UV		-		
12	M1DW	Moderna 1	D245			-		
13	P1BS	Pfizer1 (D27)	D26 (D27)	Overnight UV	-	+++(300mg/dl)	9.0	-
14	N/S	Control	D0	-	-	-	6.0	-
15	P1DW	Pfizer 1	D0	-	+/- (100mg/dl)	-	6.0	+(10RBC/μl)
16	P2DW	Pfizer 2	D0	-	+/- (100mg/dl)	-	6.0	+(10RBC/μl)
17	P4DW	Pfizer 4	D0	-	+/- (100mg/dl)	-	6.0	++(50RBC/μl)
18	M1DW	Moderna 1	D0	-	+/- (100mg/dl)	-	6.0	+(10RBC/μl)
19	M2DW	Moderna 2	D0	-	+/- (100mg/dl)	-	6.0	+(10RBC/μl)

BS = Baking Soda; NS = normal saline; DW = distilled water; GNP = colloidal Gold; EMF/5G = Electromagnetic Field exposure (wireless recharger) with 5G streaming; UV = Ultraviolet exposure; P1, 2, 4 = Pfizer; M1, 2 = Moderna vaccine; D = incubation days

Table 13
False Positive and Negative Factors in U-stick Analysis

	Glucose	Protein	pH	Occult Blood
False Positive	Hypochlorite Oxidants	Alkaline solution Ammonia Chlorohexidine (0.25%)	Bacteria → Alkaline	Hypochlorite Peroxidase
False Negative	Vt C (>50mg%) Ketone High-density solution			Vt C (>50mg%) Captopril (>100mg%)

→ = bacterial contamination triggers alkaline state

References

AGC (2021). AGC Biologics' Heidelberg Facility to Further Supply Plasmid DNA for COVID-19 Vaccine. AGC Biologics. https://www.agcbio.com/news/agc-biologics-heidelberg-facility-to-further-supply-plasmid-dna-for-covid-19-vaccine

Alamoudi, A., Celik, A., and Eltawil, A.M. (2021). Energy Efficient Capacitive Body Channel Access Schemes for Internet of Bodies," *2021 IEEE Global Communications Conference (GLOBECOM)*, https://ieeexplore.ieee.org/document/9685810

Alavi, S.H., and Kheradvar, A. (2012). Metal mesh scaffold for tissue engineering of membranes. *Tissue Eng Part C Methods*, 18(4):293-301. https://www.ncbi.nlm.nih.gov/pmc/articles/PMC3311880/

Akyildiz, I. F., and Jornet, J. M. (2010). The internet of nano-things. *IEEE Wireless Communications*, *17*(6):58-63. https://ianakyildiz.com/bwn/surveys/nanothings.pdf

Alavi, S.H., Kheradvar, A. (2012). Metal mesh scaffold for tissue engineering of membranes. *Tissue Eng Part C Methods*, 18(4):293-301. https://www.ncbi.nlm.nih.gov/pmc/articles/PMC3311880/

Anderson, M. (2022). The MAC Phenomenon and the intracorporeal network of nanocommunications: A review. *Rumble*. https://rumble.com/v15a4r1-the-mac-phenomenon-in-people-vaccinated-from-covid19.html

Bailey, M. (2022). COVID Vaccines: A Curious Discovery on the Graphene Oxide Question. Truth Comes to Light. https://drsambailey.com/resources/videos/vaccines/nz-scientist-examines-pfizer-jab-under-the-microscope/

Bailey, S. (2022). COVID Vaccines: A Curious Discovery on the Graphene Oxide Question. Dr. Sam Bailey. https://drsambailey.com/covid-vaccines-a-curious-discovery-on-the-graphene-oxide-question/

Balghusoon, A. O., and Mahfoudh, S. (2020). Routing protocols for wireless nanosensor networks and internet of nano things: a comprehensive survey. *IEEE Access*, *8*, 200724-200748. https://ieeexplore.ieee.org/stamp/stamp.jsp?arnumber=9247091

Balasubramaniam, S., and Kangasharju, J. (2013). Realizing the Internet of Nano Things: Challenges, Solutions, and Applications. *Computer, 46*, 62-68. https://www.computer.org/csdl/magazine/co/2013/02/mco2013020062/13rRUxNmPHo

Beattie, K. A. (2021). *Worldwide Bayesian Causal Impact Analysis of Vaccine Administration on Deaths and Cases Associated with COVID-19: A BigData Analysis of 145 Countries*. https://www.researchgate.net/publication/356248984_Worldwide_Bayesian_Causal_Impact_Analysis_of_Vaccine_Administration_on_Deaths_and_Cases_Associated_with_COVID-19_A_BigData_Analysis_of_145_Countries

Beattie, K.A. (2024) An Executive Summary of the Special Issue of IJVTPR — The Vaccines Were the "COVID-19 Pandemic": An Update of Beattie's Worldwide Bayesian Analysis of the Effects of the Experimental COVID-19 Injections on Deaths, Cases, and Excess Mortality in 210 Countries and 38 Regions. *International Journal of Vaccine Theory, Practice, and Research*, TBA.

Betal, S., Saha, A.K., Ortega, E., Dutta, M., Ramasubramanian, A.K., Bhalla, A.S., and Guo, R. (2018). Core-shell magnetoelectric nanorobot – A remotely controlled probe for targeted cell manipulation. *Scientific Reports, 8*, Article 755. https://doi.org/10.1038/s41598-018-20191-w

Bigtree, D. and Cole, R. (2022 December 12). The Highwire's Investigation of COVID Vaccines. *The Highwire*. https://thehighwire.com/ark-videos/the-highwires-lab-investigation-of-covid-vaccines/

Blaylock, R. L. (2021). Excitotoxicity (Immunoexcitotoxicity) as a Critical Component of the Cytokine Storm Reaction in Pulmonary Viral Infections, Including SARS-Cov-2. *International Journal of Vaccine Theory, Practice, and Research*, *1*(2), 223–242. https://doi.org/10.56098/ijvtpr.v1i2.14

Blaylock, R. L. (2022a). Responses to comments on my paper: "COVID Update: What is the truth?" *Surgical Neurology International*, *13*, 316. https://doi.org/10.25259/SNI_578_2022

Blaylock, R. L. (2022b). The COVID-19 "vaccines": What is the truth? *International Journal of Vaccine Theory, Practice, and Research*, *2*(2), 595–602. https://doi.org/10.56098/ijvtpr.v2i2.57

Burke, P., and Rutherglen, C. (2010). Toward a single-chip, implantable RFID system: Is a single-cell radio possible? Biomedical Microdevices, 12(4), 589-596. https://doi.org/10.1007/s10544-008-9266-4

Burkhardt, A. (2022) Notes and recommendations for conducting post-mortem examination (autopsy) of persons deceased in connection with COVID vaccination. doctors 4 covidethics.org https://doctors4covidethics.org/wp-content/uploads/2022/03/autopsy-directions-revised.pdf

Campra, P. (2021a). Detection of graphene in COVID 19vaccines. Counteranalysis of COVID Vaccines. https://www.researchgate.net/publication/355979001_DETECTION_OF_GRAPHENE_IN_COVID19_VACCINES

Campra, P. (2021b). Microstructures in COVID vaccines: Inorganic crystals or Wireless Nanosensors Network? Counteranalysis of COVID Vaccines. https://www.researchgate.net/publication/356507702_MICROSTRUCTURES_IN_COVID_VACCINES_inorganic_crystals_or_Wireless_Nanosensors_Network

Cao, S., Shao, J., Xia, Y., Che, H., Zhong, Z., Meng, F., van Hest, J.C.M., Abdelmohsen, L.K.E.A., Williams, D.S. (2019). Molecular Programming of Biodegradable Nanoworms via Ionically Induced Morphology Switch toward Asymmetric Therapeutic Carriers. *Small*. 15(38). https://onlinelibrary.wiley.com/doi/full/10.1002/smll.201901849

Celik, A., Khaled N. Salama, K.N., and Ahmed M. Eltawil, A.M. (2022). The Internet of Bodies: A Systematic Survey on Propagation Characterization and Channel Modelling. *IEEE Internet of Things Journal*, 9(1):321-345. https://ieeexplore.ieee.org/stamp/stamp.jsp?arnumber=9490369

Classen, J. B. (2021) COVID-19 RNA based vaccines and the risk of prion disease. *Microbiology & Infectious Diseases*, **5**, 1–3. https://principia-scientific.com/covid-19-rna-based-vaccines-and-the-risk-of-prion-disease/

Classen, J. B. (2023). Possible Treatments for COVID Vaccine induced prion disease. *Recent Advances in Clinical Trials*, *3*(2). https://doi.org/10.33425/2771-9057.1024

Cruz Alvarado, M. A., & Bazán, P. (2019). Understanding the Internet of Nano Things: overview, trends, and challenges. *E-Ciencias de la Información*, *9*(1), 152-182. https://www.redalyc.org/journal/4768/476862662008/476862662008.pdf

Dambri, O. A., Cherkaoui, S., and Makrakis, D. (2022). Design and evaluation of a receiver for wired nano-communication networks. *IEEE Transactions on NanoBioscience*. https://arxiv.org/pdf/2009.11805.pdf

Dasdag, S., Akdag, M.Z., Erdal, M.E., Erdal, N., Ay, O.I., Ay, M.E., Yilmaz, S.G., Tasdelen, B., Yegin, K. (2015). Effects of 2.4 GHz radiofrequency radiation emitted from Wi-Fi equipment on microRNA expression in brain tissue. *Int J Radiat Biol*, 91(7):555-61. https://pubmed.ncbi.nlm.nih.gov/25775055/

Dhuli, M.C. Medori, C., Micheletti, K., Donato, F., Fioretti, A., Calzoni, A., Praderio, M.G., De Angeli, G., Arabia, S., Cristoni, S., Nodari, M. (2023). Presence of viral spike protein and vaccinal spike protein in the blood serum of patients with long-COVID syndrome. *European Review for Medical and Pharmacological Sciences*, 27:13-19. https://www.europeanreview.org/wp/wp-content/uploads/013-019-2.pdf

Diblasi, L. and Sangorrin, (2024). Analysis of COVID-19 Injections — 50 Undeclared Chemical Elements, Graphene Oxide, Fluorescent Particles – Conversation with Biotechnologist Lorean Diblasi. Interview with Ana Maria Mihalcea. https://anamihalceamdphd.substack.com/p/analysis-of-covid-19-injections-50

Dubuc, B., Quiniou, J.F., Roques-Carmes, C., Tricot, C., and Zucker, S. W. (1989). Evaluating the fractal dimension of profiles. *Phys. Rev. A* 39, 39(3):1500. https://journals.aps.org/pra/abstract/10.1103/PhysRevA.39.1500

El-Husseiny, H.M., Mady, E.A., Hamabe, L., Abugomaa, A., Shimada, K., Yoshida, T., Tanaka, T., Yokoi, A., Elbadawy, M., Tanaka, R. (2022) Smart/stimuli-responsive hydrogels: Cutting-edge platforms for tissue engineering and other biomedical applications. *Materials Today Bio*. https://www.x-mol.net/paper/article/1469390524673204224

Endo, Y. (2021). Development of a cell-free protein synthesis system for practical use, *Proceedings of the Japan Academy, Series B, 2021, Volume 97, Issue 5*, Pages 261-276 https://www.jstage.jst.go.jp/article/pjab/97/5/97_PJA9705B-03/_html/-char/en

FDA. 2021. BLA Approval Letter. Food and Drug Administration. https://www.fda.gov/media/151710/download

Finn, T.M. (2011). U.S. FDA requirements for Human Vaccine Product Safety and Potency Testing *Procedia in Vaccinology*. 5:137-140. https://www.sciencedirect.com/science/article/pii/S1877282X11000282

Gat, I., Kedem, A., Dviri, M., Umanski, A., Levi, M., Hourvitz, A., Baum, M. (2022). COVID-19 vaccination BNT162b2 temporarily impairs semen concentration and total motile count among semen donors. *Andrology*, Sep;10(6):1016-1022. https://www.ncbi.nlm.nih.gov/pmc/articles/PMC9350322/

Hagimă, G. (2023a). Interview. Electron Microscopy of Comirnaty, Moderna C19 Shots, Dental Anaesthetics & Pneumovax. https://rumble.com/v3xti7w-electron-microscopy-of-comirnaty-moderna-c19-shots-dental-anestetics-and-pn.html

Hagimă, G. +(2023b). The Danger In The Air - Rainwater Analysis Research From Romania Shows Magnetic Nanoparticles And Filaments. Comparison To Clifford Carnicom's Rainwater Analysis. https://www.activenews.ro/opinii/EXCLUSIV-ActiveNews-CE-SE-AFLA-IN-APA-DE-PLOAIE-PERICOLUL-DIN-AER.-Dr.-Geanina-Hagima-Apel-catre-cercetatorii-romani-dar-si-catre-patriotii-din-structurile-de-aparare-si-informatii.-FOTO-prin-microscopie-electronica-si-VIDEO-183736

Hughes, D. A. (2022). What is in the so-called COVID-19 "vaccines"? Part 1: evidence of a global crime against humanity. *International Journal of Vaccine Theory, Practice, and Research*, *2*(2), 455–586. https://doi.org/10.56098/ijvtpr.v2i2.52

Idrees, D. and Kumar, V. (2021) SARS-CoV-2 spike protein interactions with amyloidogenic proteins: Potential clues to neurodegeneration. *Biochemical and Biophysical Research Communications*, **554**, 94–8. https://doi.org/10.1016/j.bbrc.2021.03.100

Idrees, D., Kumar, V., (2021). SARS-CoV-2 spike protein interactions with amyloidogenic proteins: Potential clues to neurodegeneration. Biochem Biophys Res Commun. 2021 May 21;554:94-98. doi: 10.1016/j.bbrc.2021.03.100

Ilori, A.O., Gbadamosi, O.A., Ibitola, G.A., Ajanaku, O. (2019). Risk Assessments of Magnetic Field Radiation from AC and Battery Powered Laptop Computers. *American Journal of Science and Technology*. 6(2):14-19. http://www.aascit.org/journal/archive2?journalId=902&paperId=7628

Jing, Y., Peng, H., and Liu, Z. (2023). WBNN: a weight-based next neighbor selection algorithm for wireless body area network. Soft Computing. 28:1803-1818. https://link.springer.com/article/10.1007/s00500-023-09511-z

Johnson, L., Broudy, D. and Hughes, D.A. (2024a) Bringing Transhumanism Down to Earth, Part 1: Military Intelligence Operations Cloaked in the False Promise of Transcendence. *Propaganda in Focus*. https://propagandainfocus.com/bringing-transhumanism-down-to-earth-part-1-military-intelligence-operations-cloaked-in-the-false-promise-of-transcendence/

Johnson, L., Broudy, D. and Hughes, D.A. (2024b) Transhumanist Futures, Part 2: Humanity in the Crosshairs. *Propaganda in Focus*. https://propagandainfocus.com/transhumanist-futures-part-2-humanity-in-the-crosshairs/

Johnson, L., Broudy, D. and Hughes, D.A. (2024c) Military Operations in Civilian Disguise, Part 3: Bio-Nano Governance and Terms of Use for Humans 2.0. *Propaganda in Focus*. https://propagandainfocus.com/military-operations-in-civilian-disguise-part-3-bio-nano-governance-and-terms-of-use-for-humans-2-0/

Johnson, L., Broudy, D. and Hughes, D.A. (2024da) WHO's Pulling the Strings? COVID Injections and the Internet of Bio-Nano Things, Part 4: Testing New Human Nodes of Connectivity. *Propaganda in Focus*. https://propagandainfocus.com/whos-pulling-the-strings-covid-injections-and-the-internet-of-bio-nano-things-part-4-testing-new-human-nodes-of-connectivity/

Jornet, J.M and Akyildiz, I.F. (2014). Graphene-based Plasmonic Nano-Antenna for Terahertz Band Communication in Nanonetworks, *IEEE Journal on Selected Areas in Communications*, 31(12):685-694. https://web.archive.org/web/20170810210901id_/http://bwn.ece.gatech.edu/papers/2014/c1.pdf

Kashani, Z.A., Pakzad, R., Fakari, F.R., Haghparast, M.S., Abdi, F., Kiani, Z., Talebi, A., Haghgoo, S.M. (2023). Electromagnetic fields exposure on fetal and childhood abnormalities: Systematic review and meta-analysis. *Open Med (Wars)*, 12;18(1):20230697. https://www.ncbi.nlm.nih.gov/pmc/articles/PMC10183723/

King Abdullah University. (2021). A network of body monitoring devices using our own tissue as the basis for the internet of bodies. Physics.Org. https://phys.org/news/2021-11-network-body-devices-tissue-basis.html

Kingston, K. 2023. (2023). mRNA is an Operating System - Technology Platform per Moderna Website. The Kingston Report. https://karenkingston.substack.com/p/mrna-is-an-operating-system-technology

Khan, T., Civas, M., Cetinkaya, O., Abbasi, N. A., and Akan, O. B. (2020). Nanosensor networks for smart health care. In *Nanosensors for Smart Cities* (pp. 387-403). *Elsevier*. https://www.researchgate.net/profile/Oktay-Cetinkaya-2/publication/339260608_Nanosensor_networks_for_smart_health_care/links/600c738292851c13fe3206c6/Nanosensor-networks-for-smart-health-care.pdf

Kyrie, V. and Broudy, D. (2022). Cyborgs R Us: The bio-nano panopticon of injected bodies? *International Journal of Vaccine Theory, Practice, and Research*, *2*(2), 355-383. https://doi.org/10.56098/ijvtpr.v2i2.49

Lee, S.J., Jung, C. A., Choi, K., and Kim, S. (2015). Design of wireless nanosensor networks for intrabody application. *International Journal of Distributed Sensor Networks, 11(7), Art. no. 176761.* http://csc.columbusstate.edu/lee/publications/IJDSN_176761-2015.pdf

Leung, W.-Y., Wu, H.H.L., Floyd, L., Ponnusamy, A., Chinnadurai, R., (2023). COVID-19 Infection and Vaccination and Its Relation to Amyloidosis: What Do We Know Currently? *Vaccines*, 11(7):1139. https://www.mdpi.com/2076-393X/11/7/1139

Li, L., Yu, Z., Liu, J., Liu, J., Yang, M., Shi, G., Feng, Z., Luo, W., Ma, H., Guan, J., Mou, F. (2023). Swarming Responsive Photonic Nanorobots for Motile-Targeting Microenvironmental Mapping and Mapping-Guided Photothermal Treatment. *Nano-Micro Lett.* 15,141 https://doi.org/10.1007/s40820-023-01095-5

Lyons-Weiler, J. (2020). Pathogenic priming likely contributes to serious and critical illness and mortality in COVID-19 via autoimmunity. *Journal of Translational Autoimmunity*, *3*, 100051. https://doi.org/10.1016/j.jtauto.2020.100051

Maervoet, V.E.T. and Briers, Y. (2017) Synthetic biology of modular proteins. *Bioengineered*, Taylor & Francis. **8**, 196–202. https://doi.org/10.1080/21655979.2016.1222993

Marik, P. (2023). Bombshell Study on Vaccine 'Ribosomal Frameshifting'. Epoch News. https://www.theepochtimes.com/epochtv/bombshell-study-on-vaccine-ribosomal-frameshifting-dr-paul-marik-atlnow-5548921?&utm_medium=AmericanThoughtLeaders&utm_source=SocialM&utm_campaign=PaulMarik&utm_content=12-18-2023

Marsudi, M.A., Ariski, R.T., Wibowo, A., Cooper, G., Barlian, A., Rachmantyo, R., Bartolo, P.J.D.S. (2021). Conductive Polymeric-Based Electroactive Scaffolds for Tissue Engineering Applications: Current Progress and Challenges from Biomaterials and Manufacturing Perspectives. *Int. J. Mol. Sci.* 22(21):11543. https://doi.org/10.3390/ijms222111543

Martin, A. (2024). *The Messenger*. Connecticut College. http://www.conncoll.edu/news/cc-magazine/past-issues/2021-issues/winter-2021/the-messenger/

Martins, N. R., Angelica, A., Chakravarthy, K., Svidinenko, Y., Boehm, F. J., Opris, I., Lebedev, M. A., Swan, M., Garan, S. A., Rosenfeld, J. V., Hogg, T., and Freitas, R. A. (2019). Human brain/cloud interface. *Frontiers in Neuroscience*, *13,* Article 112. https://doi.org/10.3389/fnins.2019.00112

McKernan, K., Helbert, Y., Kane, L. T., & McLaughlin, S. (2023). *Sequencing of bivalent Moderna and Pfizer mRNA vaccines reveals nanogram to microgram quantities of expression vector dsDNA per dose*. OSF. https://doi.org/10.31219/osf.io/b9t7m

Mead, M.N., Seneff, S., Wolfinger, R., Rose, J., Denhaerynck, K., Kirsch, S. et al. (2024a). COVID-19 mRNA Vaccines: Lessons Learned from the Registrational Trials and Global Vaccination Campaign. *Cureus*, Cureus. **16**. https://doi.org/10.7759/cureus.52876

Mead, M. N., Seneff, S., Wolfinger, R., Rose, J., Denhaerynck, K., Kirsch, S., & McCullough, P. A. (2024b). COVID-19 modified mRNA "vaccines", Part 1: Lessons learned from clinical trials, mass vaccination, and the bio-pharmaceutical complex. *International Journal of Vaccine Theory, Practice, and Research*, *3*(1), 1112–1178. https://doi.org/10.56098/fdrasy50

Mead, M. N., Seneff, S., Wolfinger, R., Rose, J., Denhaerynck, K., Kirsch, S., & McCullough, P. A. (2024c). COVID-19 modified mRNA "vaccines", Part 2: Lessons learned from clinical trials, mass vaccination, and the bio-pharmaceutical complex. *International Journal of Vaccine Theory, Practice, and Research*, *3*(1), ???

Moderna. (2022). Moderna Announces First Participants Dosed in Phase 2/3 Study of COVID-19 Vaccine Candidate in Pediatric Population. https://wikispooks.com/wiki/Moderna_COVID-19_vaccine#cite_note-9

Moon, J.H. (2020). Health effects of electromagnetic fields on children. *Clin Exp Pediatr*, 63(11):422-428. https://www.e-cep.org/journal/view.php?doi=10.3345/cep.2019.01494

Mousavi, S.M., Hashemi, S.A., Gholami, A., Mazraedoost, S., Chiang, W-H., Arjmand, O., Omidifar, N., Babapoor, A. (2021). Precise Blood Glucose Sensing by Nitrogen-Doped Graphene Quantum Dots for Tight Control of Diabetes, *Journal of Sensors*, vol. 2021 https://doi.org/10.1155/2021/5580203

Mulroney, T.E., Pöyry, T., Yam-Puc, J.C., Rust, M., Harvey, R.F., Kalmar, L. et al. (2023) N1-methylpseudouridylation of mRNA causes +1 ribosomal frameshifting. *Nature*, *625*, 189–94. https://doi.org/10.1038/s41586-023-06800-3

Murakami, H. (2023). Professor Murakami discusses cancer promoting DNA sequence in Pfizer jab. Rumble. https://rumble.com/v2m9732-malicious-prof.-murakami-discusses-cancer-promoting-dna-sequence-found-in-p.html

Noh, Y.K., Du, P., Kim, I.G., Ko, J., Kim, S.W., Park, K. (2016). Polymer mesh scaffold combined with cell-derived ECM for osteogenesis of human mesenchymal stem cells. *Biomater Res*. https://pubmed.ncbi.nlm.nih.gov/27057347/

Noor-A-Rahim, M., John, J., Firyaguna, F., Sherazi, H.H.R., Kushch, S., Vijayan, A., O'Connell, E., Pesch, D., O'Flynn, B., O'Brien, W., Hayes, M., Armstrong. E. (2022). Wireless Communications for Smart Manufacturing and Industrial IoT: Existing Technologies, 5G and Beyond. *Sensors (Basel)*. 23(1):73 https://pubmed.ncbi.nlm.nih.gov/36616671/

Nyström, S., & Hammarström, P. (2022). Amyloidogenesis of SARS-CoV-2 spike protein. *Journal of the American Chemical Society*, *144*(20), 8945–8950. https://doi.org/10.1021/jacs.2c03925

Perez, J.-C., Moret-Chalmin, C. and Montagnier, L. (2023) Emergence of a new Creutzfeldt-Jakob Disease: 26 cases of the human version of Mad-Cow Disease, a few days after a COVID-19 injection. *International Journal of Vaccine Theory, Practice, and Research*, **3**, 727–70. https://doi.org/10.56098/ijvtpr.v3i1.66

Reuters. (2021, February 9). Fact check: The COVID-19 vaccine is not an operating system designed to program humans. *Reuters*. https://www.reuters.com/article/world/fact-check-the-covid-19-vaccine-is-not-an-operating-system-designed-to-program-idUSKBN2A912Y/

Russell, C.L. (2018). 5G wireless telecommunications expansion: Public health and environmental implications. *Environ Res*, 165:484-495. https://pubmed.ncbi.nlm.nih.gov/29655646/

Santiago, D. (2022). Playing Russian Roulette with every COVID-19 injection: The deadly global game. *International Journal of Vaccine Theory, Practice, and Research*, *2*(2), 619–650. https://doi.org/10.56098/ijvtpr.v2i2.36

Santiago, D. and Oller, J.W. (2023) Abnormal clots and all-cause mortality during the pandemic experiment: five doses of COVID-19 vaccine are evidently lethal to nearly all Medicare participants. *International Journal of Vaccine Theory, Practice, and Research*, **3**, 847–90. https://doi.org/10.56098/ijvtpr.v3i1.73

Segalla, G. (2023a). Adjuvant activity and toxicological risks of lipid nanoparticles contained in the COVID-19 "mRNA vaccines." *International Journal of Vaccine Theory, Practice, and Research*, *3*(1), 1085–1102. https://doi.org/10.56098/z1ydjm29

Segalla, G. (2023b). Apparent cytotoxicity and intrinsic cytotoxicity of lipid nanomaterials contained in a COVID-19 mRNA vaccine. *International Journal of Vaccine Theory, Practice, and Research*, *3*(1), 957–972. https://doi.org/10.56098/ijvtpr.v3i1.84

Segalla, G. (2023c). Chemical-physical criticality and toxicological potential of lipid nanomaterials contained in a COVID-19 mRNA vaccine. *International Journal of Vaccine Theory, Practice, and Research*, *3*(1), 787–817. https://doi.org/10.56098/ijvtpr.v3i1.68

Seneff, S., Nigh, G., Kyriakopoulos, A.M., McCullough, P.A. (2022). Innate immune suppression by SARS-CoV-2 mRNA vaccinations: The role of G-quadruplexes, exosomes, and MicroRNAs. *Food and Chemical Toxicology*, 164. https://www.sciencedirect.com/science/article/pii/S027869152200206X?via%3Dihub

Shah KV. SV40 and human cancer: a review of recent data. Int J Cancer. 2007 Jan 15;120(2):215-23. doi: 10.1002/ijc.22425. PMID: 17131333.

Shaw, C. A. (2017). *Neural Dynamics of Neurological Disease*. John Wiley & Sons, Inc. https://doi.org/10.1002/9781118634523.refs

Shiu, B.C., Liu, Y.L., Yuan, Q.Y., Lou, C.W., Lin, J.H. (2022). Preparation and Characterization of PEDOT:PSS/TiO_2Micro/Nanofiber-Based Gas Sensors. *Polymers (Basel)*. 14(9):1780. https://pubmed.ncbi.nlm.nih.gov/35566945/

Spectroscopy and Campra, P. (2021) Detection of graphene in COVID-19 vaccines. https://www.researchgate.net/publication/355979001_DETECTION_OF_GRAPHENE_IN_COVID19_VACCINES

Suberi, A., Grun, M. K., Mao, T., Israelow, B., Reschke, M., Grundler, J., Akhtar, L., Lee, T., Shin, K., Piotrowski-Daspit, A.S., Homber, R.J., Iwasak, A., Suh, H.W., and Saltzman, W.M. (2023). Polymer nanoparticles deliver mRNA to the lung for mucosal vaccination. *Science Translational Medicine*, *15*(709), DOI: 10.1126/scitranslmed.abq0603

Truong, N.P., Quinn, J.F., Whittaker, M.R., and Davis, T.P. (2016). Polymeric filomicelles and nanoworms: two decades of synthesis and application. *Polymer Chemistry*, 26. https://pubs.rsc.org/en/content/articlelanding/2016/py/c6py00639f

Vojdani, A., & Kharrazian, D. (2020). Potential antigenic cross-reactivity between SARS-CoV-2 and human tissue with a possible link to an increase in autoimmune diseases. *Clinical Immunology (Orlando, Fla.)*, *217*, 108480. https://doi.org/10.1016/j.clim.2020.108480

Vojdani, A., Vojdani, E., & Kharrazian, D. (2021). Reaction of human monoclonal antibodies to SARS-CoV-2 proteins with tissue antigens: Implications for autoimmune diseases. *Frontiers in Immunology*, *11*, 617089. https://doi.org/10.3389/fimmu.2020.617089

WHO, World Health Organization. 2021. WHO Laboratory Manual for the Examination and Processing of Human Semen. Sixth Edition. https://iris.who.int/bitstream/handle/10665/343208/9789240030787-eng.pdf?sequence=1

Woodruff, K. and Maerkl, S.J. (2016) A high-throughput microfluidic platform for mammalian cell transfection and culturing. *Scientific Reports*, Nature Publishing Group. **6**, 23937. https://doi.org/10.1038/srep23937

Xie, Y., Kawazoe, N., Yang, Y., and Chen, G. (2021). Preparation of mesh-like collagen scaffolds for tissue engineering. *Materials Advances, 3*, 1556-1564. https://pubs.rsc.org/en/content/articlelanding/2022/MA/D1MA01166A

Zhang, S., Chen, Y., Liu, H., Wang, Z., Ling, H., Wang, C. et al. (2020) Hydrogels: room-temperature-formed PEDOT:PSS hydrogels enable injectable, soft, and healable organic bioelectronics. *Advanced Materials*, **32**, 2070005. https://doi.org/10.1002/adma.202070005

Zhou, H., Mayorga-Martinez, C.C., Pané, S., Zhang, L., and Pumera, M. (2021). Magnetically Driven Micro and nanorobots. Chemical Reviews 121(8):4999-5041. https://pubs.acs.org/doi/10.1021/acs.chemrev.0c01234